KINETICS OF SELECTIVE CO OXIDATION IN HYDROGEN-RICH STREAMS OVER Pt-Co-Ce/Al_2O_3 CATALYST

by

Göktuğ Nezihi Özyönüm

B. S. in Ch.E., Yıldız Technical University, 2002

Submitted to the Institute for Graduate Studies in
Science and Engineering in partial fulfillment of
the requirements for the degree of
Master of Science

Graduate Program in Chemical Engineering

Boğaziçi University

2005

to my family

ACKNOWLEDGEMENTS

Firstly, I would like to express my sincere thanks to my thesis supervisor, Assoc. Prof. Ramazan Yıldırım, who has given continuous encouragement, support and trust. I am grateful to him for his patience.

My sincere gratitude is due to my thesis committee members, Prof. Ayşe Nilgün Akın and Assoc. Prof. Ahmet Erhan Aksoylu who have read and commented on my thesis.

Special thanks to Gökhan Uysal, Eyüp Şimşek, Şeyma Özkara, Burcu Selen Çağlayan, Feyza Gökaliler, and Tuğçe Gözaçan for giving me their friendship. Their friendship and support has given me strength.

Cordial thanks for Bilgi Dedeoğlu, Nurettin Bektaş and Yakup Bal for their technical assistance and help.

Finally, I wish to thank my family for their support throughout my entire education. This thesis would not have been possible without them.

Financial support provided by the Boğaziçi University Research Fund through project BAP04M105 and by the Scientific and Technical Research Council of Turkey through project MISAG-228 is gratefully acknowledged.

ABSTRACT

KINETICS OF SELECTIVE CO OXIDATION IN HYDROGEN-RICH STREAMS OVER $Pt\text{-}Co\text{-}Ce/Al_2O_3$ CATALYST

Kinetics of low temperature CO oxidation was studied in hydrogen-rich streams with a realistic gas composition using cobalt and ceria promoted Pt/Al_2O_3 catalyst prepared by incipient-to-wetness impregnation. All plausible elementary reactions constituting the CO oxidation mechanism were determined and five alternative mechanisms based on those elementary reactions were constructed. The mechanisms comprise of two single site monofunctional paths proceeding on the platinum sites, and three dual site bifunctional paths proceeding on the platinum sites and the cobalt-ceria sites. Both the cobalt and the ceria sites are referred to by a single site for simplicity. H_2, CO_2 and H_2O in the feed stream were not included in the reaction mechanisms, as their effect on the reaction rates were considered to be through the rate parameters, but not through the reaction mechanism. Intrinsic kinetic data were obtained in the initial rate region in a microflow reactor operating in differential mode using eight different sets of CO and O_2 concentrations each at two space times, i.e. two catalyst loadings, at 110 °C both in the presence of 25 per cent CO_2 and 10 per cent H_2O, and in the absence of CO_2 and H_2O. The effect of temperature on the reaction rates was also investigated in the range of 110-130 °C. The experimental rate data were used to estimate the kinetic parameters of the model equations for the mechanisms proposed in this study, and for six alternative mechanisms from other studies in the literature. Model discrimination between all the model equations tested was carried out by comparing the calculated data with the experimental data. Five models, i.e. one monofunctional, three bifunctional models and one model without a proposed mechanism, were chosen as the plausible kinetic models among the eleven models, as no distinction could be made between them statistically.

ÖZET

HİDROJENCE ZENGİN GAZ KARIŞIMLARINDA $Pt\text{-}Co\text{-}Ce/Al_2O_3$ KATALİZÖRÜ ÜZERİNDE SEÇİCİ KARBON MONOKSİT OKSİDASYONU KİNETİĞİ

Emdirme yöntemi ile hazırlanmış Co ve Ce katkılı Pt/Al_2O_3 katalizörü kullanılarak hidrojence zengin ve gerçekçi bir gaz bileşiminin sağlandığı bir ortamda düşük sıcaklık karbon monoksit oksidasyonu kinetiği çalışılmıştır. Karbon monoksit oksidasyonu mekanizmasını oluşturan tüm makul elementer reaksiyonlar belirlenmiş ve elementer reaksiyonlara dayalı beş farklı mekanizma kurulmuştur. Mekanizmalar, platin mevkileri üzerinde yürüyen iki tek mevkili, tek-işlevli, ve platin ve Co-Ce mevkileri üzerinde yürüyen üç çift mevkili, çift-işlevli yoldan oluşmaktadır. Kolaylık amacıyla, hem Co, hem de Ce mevkileri tek bir mevkiiyle gösterilmiştir. Besleme akımındaki hidrojen, karbon dioksit ve su buharının, reaksiyon mekanizmasını değil, hız parametrelerini etkilediği kabul edilerek, bu bileşenlerin girdiği reaksiyonlar reaksiyon mekanizmalarına dahil edilmemiştir. Kinetik veriler, diferansiyel biçimde çalışan bir mikroakış reaktörü içinde, her biri iki boşluk zamanında, yani iki katalizör yüklemesinde, sekiz farklı grup karbon monoksit ve oksijen konsantrasyonu kullanılarak 110 °C'de, hem yüzde 25 karbon dioksit ve yüzde 10 su buharının varlığında, hem de karbon dioksit ve su buharının yokluğunda elde edilmiştir. Ayrıca, sıcaklığın reaksiyon hızları üzerine etkisi 110-130 °C aralığında araştırılmıştır. Deneysel hız verileri, bu çalışmada oluşturulan beş, ve literatürde önerilen altı farklı mekanizmanın model denklemlerinin kinetik parametrelerinin hesaplanmasında kullanılmıştır. Test edilen tüm model denklemleri arasındaki ayrım, hesaplanan verilerle deneysel verilerin kıyaslanmasıyla gerçekleştirilmiştir. On bir model arasından, biri tek-işlevli, üçü çift-işlevli ve biri mekanizmasız olmak üzere beş model, aralarında istatistiksel olarak bir ayrım yapılamadığından dolayı, makul kinetik modeller olarak seçilmiştir.

TABLE OF CONTENTS

LIST OF FIGURES

LIST OF TABLES

LIST OF SYMBOLS/ABBREVIATIONS

b	Parameter vector
F_{CO}	CO flow
k_i^b	Rate constant of backward reaction of step i
k_i^f	Rate constant of forward reaction of step i
K_i	Equilibrium constant of reaction step i
n	Number of experiments
P_i	Partial pressure of component i
P_t	Total pressure
r_i	Reaction rate according to component i
R^2	Regression coefficient
S	Objective function
T	Temperature
$v_{i,j}$	Stoichiometric coefficient of surface species i in reaction step j
W_{CAT}	Weight of catalyst
X_{CO}	CO conversion
x_i	Vector of set variables for experiment i
y_i	*i*th experimental observation
σ_i	Stoichiometric coefficients for elementary steps of path i
$\Delta H°$	Enthalpy of the reaction at the standart conditions
$\theta_{O\bullet}$	Coverage of adsorbed oxygen on ceria sites
AFC	Alkaline Fuel Cell
DRIFTS	Diffuse Reflectance Infrared Fourier Transform Spectroscopy
ER	Eley–Rideal
FCC	Fluid Catalytic Cracking
FTIR	Fourier Transform Infrared
GC	Gas Chromatograph

HPLC	High Performance Liquid Chromatography
LH	Langmuir–Hinshelwood
MCFC	Molten Carbonate Fuel Cell
NMRO	Noble Metal Reducible Oxide
OSC	Oxygen Storage Capacity
PAFC	Phosphoric Acid Fuel Cell
PEMFC	Proton Exchange Membrane Fuel Cell
PNGV	Partnership for A New Generation of Vehicles
PEM	Polymer Electrolyte Membrane
PROX	Preferential Oxidation
SDC	Samaria-Doped Ceria
SMSI	Strong Metal Support Interaction
SOFC	Solid Oxide Fuel Cell
TCD	Thermal Conductivity Detector
TWC	Three-Way Catalysis
UHV	Ultra High Vacuum
WGS	Water-Gas Shift Reaction

1. INTRODUCTION

Environmental and public health problems stemming from automotive and power generation sources, in addition to energy supply diversification and security issues, have pushed forward the new ideas for energy production. As a result, the development of fuel-efficient engines that use lightweight materials and produce less pollutants has been a major objective for many years. One of the most promising alternatives is the fuel cell powered electrically driven vehicles which offer significant advantages compared to conventional technologies like combustion.

A fuel cell is an electrochemical device that combines a fuel and an oxidant to produce electricity. The fuel is typically hydrogen and the oxygen is oxidant resulting in water and heat as the by-product. The conversion of the fuel hydrogen to energy takes place without combustion; therefore, the process is highly efficient, clean and quiet. Fuel cells possess the necessary specific power, power density and durability to replace conventional internal combustion engines of transportation vehicles (Gray and Frost, 1998). Among the various types of fuel cells, the low temperature, H_2-fuelled, Proton Exchange Membrane Fuel Cells (PEMFCs) seem to be the most promising energy conversion system for such purpose (Avgouropoulos *et al.,* 2002). Today's test fleet of fuel cell cars, trucks and buses are powered by PEMFC.

The choice of fuel and fuel processing technology will be the fundamental factor in the success of fuel cell powered vehicles. Pure hydrogen is the ideal fuel for the PEMFC, because hydrogen is the lightest, the simplest and the most abundant element in nature. It can be both produced and utilized in an emission free manner. However, the technologies for safe, efficient and cost effective hydrogen production have not been fully developed yet (Kamarudin *et al.,* 2004).

Recent studies performed on on-board hydrogen production focus on three production routes; (i) steam reforming, (ii) partial oxidation, and (iii) indirect partial oxidation. In all cases, the resulting gas mixture contains significant amounts of CO and it is further processed in a water-gas shift (WGS) reactor. In this way, the gas stream

becomes richer in H_2 and the concentration of CO drops to lower values. The typical composition of reactant gas stream (effluent from a WGS converter placed after the reformer) is 45-75 volume per cent H_2, 15-25 volume per cent CO_2, 0.5-2 volume per cent CO, a few volume per cent H_2O and N_2. Unfortunately, even this low CO concentration cannot be tolerated by the PEMFCs, which are highly sensitive towards even the trace CO contamination in the H_2 feed gas. It is thus imperative to purify further the hydrogen feed gas reducing the CO concentration to several ppm level (Avgouropoulos *et al.*, 2002).

There are many possible strategies to accomplish the CO removal; palladium-based membranes, methanation, absorption and selective oxidation. Of these methods, preferential CO oxidation (PROX) appears to be the most promising and lowest cost approach (Manasilp and Gulari, 2002). As typical of catalytic reactions, the challenges in PROX process are to increase activity, selectivity, stability and to reduce cost. The conversion of CO has to be 99.9 per cent in order to achieve a concentration of 10 ppm. Since the PROX unit is placed between the low-temperature shift reactor (~200 ^{o}C) and the PEM fuel cell (~80 ^{o}C), it should operate between these temperatures. At the same time, the reformate is mostly hydrogen and its oxidation decreasing the overall fuel efficiency has to be hindered (Kahlich *et al.,* 1997). The selective CO oxidation catalyst must meet all these requirements.

Conventional catalysts are not active at low temperatures. An efficient low temperature CO oxidation catalyst should accommodate both CO chemisorption and the simultaneous dissociative adsorption of O_2. This has suggested the use of composite materials with different components each having activity for one of these functions (Trimm and Önsan, 2001). A series of catalysts and supports have been investigated in order to determine suitable catalysts for the selective oxidation of carbon monoxide in hydrogen-rich streams. Catalysts used for low-temperature CO oxidation in hydrogen-rich streams generally consist of a noble metal, i.e. platinum, palladium, ruthenium, etc., a reducible metal oxide, i.e. transition metal oxides, etc., and the support material.

Continual investigations of selective CO oxidation are being performed mostly related to new catalyst types and effects of different parameters on the process. However, recent efforts are deficient of kinetic studies on PROX.

The foregoing pleads are for kinetic modeling on the basis of elementary steps because of the larger impact of such models. An even more important advantage of elementary step modeling is that a model can be determined experimentally for one global reaction, but applied in a combination of elementary step kinetics for other global reactions. Modeling via elementary steps also allows adapting the kinetic model when the catalyst formulation is changed in order to introduce new catalytic functions (Hoebink *et al.,* 2001).

The Pt-Co-Ce/γ-Al_2O_3 catalyst used in the present study was first prepared and optimized by İnce (2004) in the absence of CO_2 and H_2O, and the effects of CO_2 and water vapor on the selective CO oxidation performance was studied by Uysal (2005). The catalyst was found to be successful in terms of CO oxidation activity and selectivity both in the absence and presence of CO_2 and H_2O in the feed stream even at low temperatures.

In this work, kinetics of low temperature CO oxidation was studied in hydrogen-rich streams with realistic gas compositions over Pt-Co-Ce/γ-Al_2O_3 catalyst which was prepared by impregnation method. Firstly, possible alternative CO oxidation mechanisms based on elementary reaction steps were proposed and rate expressions for each of the corresponding models were built. The second part consisted of rate calculations performed with varying reactant compositions both in the absence and the presence of CO_2 and H_2O, and the rate data were used to obtain the kinetic parameters for the model equations. The effect of temperature on the reaction rates was also investigated. Finally, discrimination between the models proposed both in this study and the other studies in the literature was carried out by comparing the calculated data with the experimental data.

Chapter 2 contains a literature survey on fuel cells, selective CO oxidation as well as a brief account on the types and properties of catalysts used. The reaction mechanisms for CO oxidation, and the methods for kinetic analysis are also examined in detail in Chapter 2. Chapter 3 describes the experimental procedure which was followed during this study. The results obtained in the experiments are presented and discussed in Chapter 4, while the conclusions and recommendations for future work are summarized in Chapter 5.

2. LITERATURE SURVEY

2.1. Fuel Cells

During the last decade, there has been a significant increase in the level of worldwide concern regarding both the release of greenhouse gases into the atmosphere, and the poor air quality in many of the world's metropolitan areas. The transportation sector, and in particular the internal combustion engine is known to be a major source of both CO_2 and the noxious gaseous emissions. Against such a backdrop of environmental and health concerns, fuel cells are now being recognized as increasingly realistic clean alternatives for motive propulsion (Dudfield *et al.,* 2001). A fuel cell is defined as an electrochemical device in which the chemical energy stored in a fuel is converted directly into electricity. A fuel cell consists of two thin electrodes (porous anode and cathode), and an ion conducting electrolyte material which is sandwiched in between the electrodes. The fuel, commonly hydrogen, is supplied to the anode while an oxidant, commonly oxygen, is supplied to the cathode generally by feeding air. On the basis of the electrolyte employed, there are five types of fuel cells. They differ in the composition of the electrolyte and are in different stages of development. They are alkaline fuel cells (AFC), phosphoric acid fuel cells (PAFC), proton-exchange membrane fuel cells (PEMFC), molten carbonate fuel cells (MCFC), and solid oxide fuel cells (SOFC) (Song, 2002).

All fuel cells have the same basic operating principle. An input fuel is catalytically reacted (electrons removed from the fuel elements) in the fuel cell to create an electric current. The input fuel passes over the anode (negatively charged electrode) where it catalytically splits into electrons and ions, and oxygen passes over the cathode (positively charged electrode). The electrons go through an external circuit to serve an electric load while the ions move through the electrolyte toward the oppositely charged cathode, at the cathode, ions combine to create by-products, primarily water and CO_2. Depending on the input fuel and electrolyte, different chemical reactions will occur (Song, 2002).

Fuel cells are alternative and new energy sources of the energy sector, because of the higher efficiency and of no emission of pollutants. Especially, the low-temperature, H_2-

fuelled, polymer electrolyte membrane fuel cells (H_2-PEMFCs) seem to be the most technically advanced fuel cell types. The ideal fuel for the PEMFCs is pure hydrogen; however, there has been no economically feasible way of storing pure hydrogen (Avgouropoulos *et al.*, 2002). On-board hydrogen production should be the most practical way to feed the cell, as no infrastructure for handling and distribution of this fuel is currently available; thus, fuels such as methane, methanol or gasoline must be reformed to obtain a hydrogen-rich gas mixture via a fuel processor (Panzera *et al.,* 2004).

The fuel processor used to supply hydrogen to a PEMFC for stationary applications normally consists of several units: a desulfurizer, a catalytic steam reformer, and a two-stage water-gas shift (WGS) reactor. The gas at the outlet of the WGS reactor typically contains 0.5–1 vol.% CO (Park *et al.,* 2004). This is because the water gas shift reaction is a reversible and equilibrium reaction, so CO cannot be removed completely (Tanaka *et al*., 2003). Unfortunately, trace amounts of CO in the H_2-PEMFC causes a devastating deterioration of the energy conversion efficiency of the fuel cell via CO-induced poisoning of the anode catalyst (Kahlich *et al.,* 1997). Therefore, the hydrogen production system must be equipped with a CO removal system. For this reason, The Partnership for a New Generation of Vehicles (PNGV), which is a broad partnership between the U.S. government, industry, universities and national laboratories, sets the CO concentration target for the fuel processor to 10 ppm or less (Son *et al.,* 2002).

2.2. Selective CO Oxidation in H_2-Rich Streams

Palladium-based membrane purification, methanation, and selective CO oxidation are the methods of reducing the CO in the feed to 10 ppm or less, to operate the fuel cell with minimal loss of hydrogen. Of these three methods, selective CO oxidation is the most promising and lowest cost approach (Manasilp and Gulari, 2002). For the academic community, this reaction is of interest due to richness of its spatio-temporal kinetics exhibiting bistability, oscillations, and pattern formation (Carlsson *et al.,* 2005).

In the selective CO oxidation reaction system, the following two oxidation reactions occur (Choi and Stenger, 2004).

Desired Reaction : $CO + ½ O_2 \longrightarrow CO_2$; $\Delta H^o = -283$ kJ/mol (2.1)

Undesired Reaction : $H_2 + ½ O_2 \longrightarrow H_2O$; $\Delta H^o = -242$ kJ/mol (2.2)

Typical of catalytic reactions, the challenges for the selective CO oxidation are activity, selectivity, stability and cost. The conversion of CO has to be 99.9 per cent in order to achieve a concentration of 10 ppm. Since the PROX unit is placed between the low-temperature WGS reactor (~200 °C) and the PEMFC (~80 °C), it should operate between these temperatures. At the same time, the reformate is mostly hydrogen and its coincident oxidation obviously decreases the overall fuel efficiency (Epling *et al.,* 2003).

PROX system operation at low temperature (room temperature) is also very important for start-up in transportation application fuel cells (Son *et al.,* 2002). More than 80 per cent of the emissions from cars equipped with catalysts arise from the first three minutes of driving. Therefore, substantial efforts are made to develop catalysts possessing high activity at cold-start conditions (Törncrona *et al.,* 1997).

2.3. Catalyst Selection for Selective CO Oxidation

The need for purification of hydrogen feed gas reducing the CO concentration to 10 ppm or less has triggered an intense research effort to develop catalysts that are able to selectively oxidize CO in the presence of excess hydrogen in the last few years (Avgouropoulos *et al.,* 2002). Park *et al*. (2005) states that the most important requirements of a catalyst for the selective oxidation of CO in excess hydrogen atmosphere are:

i. high CO oxidation activity at low temperatures
ii. good selectivity against the undesired H_2 oxidation
iii. wide temperature window of CO conversion greater than 99 per cent
iv. tolerance for the CO_2 and H_2O in the feed.

Park *et al.* (2004) reported that the catalysts proposed for the selective CO oxidation so far are mainly based on the precious metals supported on alumina, zeolites, and base metal oxides. Precious metal-based catalysts, although having a good activity for CO

oxidation, are disadvantageous with regards to high cost, limited availability, and the decrease of the selectivity at high temperatures. Besides, most conventional catalysts are not active at low temperatures and low O_2/CO ratios because O_2 and CO compete for the same sites. O_2 has more severe site requirements to dissociate over. However, CO adsorption dominates the metal surface and prevents O_2 adsorption and surface reaction. Over base metal oxide catalysts, on the other hand, O_2 is held too strongly to be displaced by CO at low temperatures. Thus, an efficient low-temperature CO oxidation catalyst should accommodate both CO chemisorption and the simultaneous dissociative adsorption of O_2. This has suggested the use of composite materials with different components, each having activity for one or other of these functions. Noble metal reducible oxide combinations, base metal oxides, and perovskite type catalysts have been tested for their low-temperature CO oxidation performance (Trimm and Önsan, 2001).

In recent years, there has been a considerable interest in the use of catalysts which contain both noble metals and metal oxides. Noble Metal Reducible Oxide (NMRO) catalysts, which have two active sites, seem to provide a promising choice for effective CO oxidation. These catalysts are produced by using one or two zero-valent noble metals (Pt, Pd, Au, Rh) with metal oxides (SnO_2, MnO_x, Fe_2O_3, CeO_x, CoO_x), which have variable valency states that can be easily reduced under reaction conditions, and distributing them over a support such as Al_2O_3 or SiO_2. None of the separate components (the noble metals or the reducible oxides) have appreciable activity for CO oxidation at low temperatures (below 150 °C) individually under practical conditions, and thus, a synergistic interaction is present in the two-component materials. Although the mechanisms of CO oxidation over these materials are not known in detail, a probable explanation for their low-temperature activity is that the noble metal chemisorbs CO and the reducible oxide provides sites that dissociatively adsorb O_2 (Özdemir, 2003). Since CO and O_2 do not compete for the same adsorption sites, the inhibition of low-temperature CO oxidation by CO itself is eliminated (Akın *et al*., 2001).

Noble metal reducible oxide catalysts used for low temperature CO oxidation must exhibit strong metal-support interaction (SMSI). One or more of three types of synergetic interaction between the two catalyst components are said to be responsible for the high efficiency observed at low temperatures (Trimm and Önsan, 2001):

i. The two components may each have independent functions in the catalytic CO oxidation mechanism
ii. The properties of one component may be modified by the presence of the other
iii. The two components may associate at the atomic level such a way as to form unique active sites.

2.3.1. Platinum (Pt) Catalysts

The oxidation of carbon monoxide over precious metals, e.g. platinum, is probably one of the most studied catalytic reactions, beginning already with the pioneering work by Langmuir in 1922. The role as a key step in many industrial processes and the importance in pollution control for stationary and mobile applications motivates further studies of this reaction. Even though the literature on the subject is extensive, there is still a need to further clarify the reaction mechanism, particularly under transient conditions, e.g. ignition and extinction (Carlsson *et al.,* 2004).

Pt catalysts can be used for the PROX due to their higher activity around 200 °C with the lower CH_4 formation rate. However, to satisfy start-up conditions in a transportation fuel cell, lower activity below 100 °C should be improved. The lower temperature activity and selectivity could be improved using smaller particles, promoters (Fe, Ce or Co), formed alloys (PtSn), sol–gel preparation, or acidic support to overcome startup problems (Son *et al.,* 2003).

Zhdanov and Kasemo (2003) stated that CO oxidation on the Pt-group metals was generally accepted to occur via the following mechanisms:

Reversible CO adsorption

$$CO_{gas} \longleftrightarrow CO_{ads} \qquad (2.3)$$

Dissociative O_2 adsorption

$$(O_2)_{gas} \longrightarrow 2O_{ads} \qquad (2.4)$$

Langmuir–Hinshelwood (LH) reaction between adsorbed CO and O

$$CO_{ads} + O_{ads} \longrightarrow (CO_2)_{gas} \quad (2.5)$$

Eley–Rideal (ER) reaction between gas-phase CO and adsorbed O

$$CO_{gas} + O_{ads} \longrightarrow (CO_2)_{gas} \quad (2.6)$$

Surface-science-based studies have shown that the ER step actually does not occur at least under ultra-high vacuum (UHV) conditions. Carlsson *et al*. (2004) stated that CO is adsorbed associatively and starts to be desorbed rapidly above about 350 K, while O_2 is adsorbed dissociatively above about 100 K and desorbed associatively above 720 K. CO diffuses rapidly over the surface and reacts with O to yield CO_2, which is immediately desorbed into the gas phase (CO_2 is desorbed at 95 K).

Mariño *et al.* (2004) reported that, among the noble metals they studied, platinum were shown to be active in the oxidation of carbon monoxide in the presence of large excess in hydrogen. High activities were measured even at low temperatures (T < 100 ºC). Unfortunately, platinum may adsorb all the reactants involved in the CO preferential oxidation. As a result, the undesired hydrogen oxidation reaction also proceeds in competition with the oxidation of CO. In fact, as the reaction temperature increases, the hydrogen oxidation becomes faster than the CO oxidation reaction and, at some point, a decrease of the selectivity towards CO_2 formation was systematically observed. Furthermore, since the oxygen activation takes place easily on these metals, the hydrogen oxidation rate is also accelerated when the oxygen concentration in the feed increases.

The reported high selectivity on platinum can easily be rationalized by the blocking action of adsorbed carbon monoxide, thereby reducing the rate of hydrogen adsorption and oxidation. Since an increase in reaction temperature is concomitant with an increase in the CO desorption rate, the selectivity is expected to decrease with temperature, as for Pt/Al_2O_3. Similarly, a decrease in the CO concentration should decrease its equilibrium surface concentration, again leading to a reduced selectivity (Kahlich *et al.,* 1997). Kwak *et al.* (2005) stated that hydrogen exerts a promotion effect on the oxidation of carbon monoxide at the region of carbon monoxide removal and a negative effect at higher temperatures, but the extent is relatively small. Therefore, the point of the problem in the

catalyst is not the selectivity for carbon monoxide removal, but the activity for the low temperature reaction.

Temperature and pressure are important variables that can significantly affect surface kinetic parameters and consequently affect reaction rate and selectivity. Temperature has an effect on every step of reaction (surface reactions, adsorption, and desorption) whereas pressure can affect the reaction in terms of the driving force to form product. Since CO oxidation is highly exothermic, operating on an industrial scale can result in temperature gradients that affect the local activity and selectivity of the catalyst. At relatively low temperatures, i.e. 90 ºC, Pt surface is predominantly covered with adsorbed CO and the rate of reaction is directly proportional to oxygen partial pressure. The relationship between selectivity and temperature for this reaction on Pt catalysts is still not clear (Sirijaruphan *et al*., 2004).

Oh and Sinkevitch (1993) observed a maximum in CO conversion with temperature on 0.5 per cent Pt/Al_2O_3 at 473 K in the presence of excess hydrogen in the feed stream. In contrast, a constant conversion of 100 per cent (above 473 K) was observed in absence of hydrogen. Kachlich *et al*. (1997) also reported that the Pt-based catalysts tested thus far achieve maximum conversions at approximately 200 ºC, with selectivity approaching 40–60 per cent in 1 per cent CO, 1 per cent O_2, and H_2 balance mixture.

Igarashi *et al*. (1997) investigated the PROX reaction on zeolite-supported Pt catalysts. Preliminary studies on Pt/A-zeolite catalyst showed extremely promising results, an order of magnitude higher CO oxidation selectivity (as compared to Pt/Al_2O_3) was obtained at similar conversion levels. Subsequent studies involving a series of catalysts (Pt/A, Pt/mordenite, Pt/X, Pt/Al_2O_3) showed that the Pt/mordenite catalyst required the least amount of excess oxygen for the complete conversion of CO (1 per cent) in presence of excess of hydrogen. The selectivity for CO oxidation versus H_2 oxidation follows the order of zeolite A > mordenite > zeolite X > alumina. Use of a two-stage reactor further increased the effectiveness of the Pt/mordenite catalyst. Also, the catalyst performance was not significantly influenced by the presence of water in the feed stream.

Schubert *et al*. (2001) have recently reported superior CO oxidation activity and selectivity (than Pt/Al_2O_3) for a bimetallic carbon-supported Pt-Sn system at low temperatures (273–353 K). Unlike the case of Pt/Al_2O_3, the CO oxidation reaction was not limited by CO desorption for the carbon-supported Pt-Sn catalysts. Based on their spectroscopic studies, the authors proposed a mechanistic model involving competitive adsorption of CO and H_2 on Pt sites, and O_2 adsorption mainly on Sn sites and SnO_x islands present in the vicinity of the active Pt-Sn particles (Choudhary and Goodman, 2002).

Korotkikh and Farrauto (2000) reported that Pt/γ-alumina catalyst promoted with Fe oxide deposited on a ceramic monolith was to be highly active, selective, and stable for the CO oxidation reaction in the presence of excess H_2 at temperatures compatible with the PEM fuel cell. The catalyst is now widely used in fuel processors, fuel cells and industrial gas generators. The presence of the Fe promoter significantly enhances the activity of the catalyst compared to a Pt only catalyst (Liu *et al*., 2002).

2.3.2. Cerium Oxide (CeO_x) Promoters

Ceria has been considered as one of the most important rare earth element in catalysis. It plays an important role in three-way catalysis (TWC) and fluid catalytic cracking (FCC). Therefore, much effort has been dedicated to studying the role of ceria (Roh *et al.,* 2004). Ceria and other base-metal oxides are normally used as oxygen storage components in TWC catalysts to damp out rapid changes in the exhaust gas, i.e. to provide oxygen under rich conditions and store oxygen under lean conditions, hence facilitating a reasonable time response for the engine-exhaust feedback system. The choice of a metal oxide depends on its ability to rapidly change oxidation states upon change in redox potential of the exhaust gas composition. The change in oxidation state is associated with the reversible removal and addition of oxygen, hence, with the designation “oxygen storage” component.

Ceria is by far the most commonly used oxygen storage component, and there are numerous experimental and theoretical studies of the oxygen storage in ceria catalysts. The oxygen storage is commonly believed to occur via oxygen surface diffusion to and from

the noble metal particle. However, the connection between experiments and calculations is relatively weak. The surface diffusion of oxygen on ceria, and the way oxygen is communicated between ceria and the catalyst particles, which are key parameters, are not well known. This is in part due to the complexity of the system, which prevents the use of many analytical tools otherwise employed in surface science studies on well-defined model systems (Johansson *et al.,* 2001).

Ceria is a crucial component of automotive, three-way, emissions-control catalysts, in part because it promotes precious-metal catalysts for the WGS reaction. While, this has been known for many years, the need for active WGS catalysts for nontraditional applications, such as fuel processing for fuel cells, has lead to renewed interest in examining ceria-supported metals for this application. Because, the activity and stability of ceria-supported catalysts is a strong function of preparation conditions, gaining insights into the mechanism and limiting steps for this reaction is important for the development of better catalysts (Hilaire *et al.,* 2001).

Noble metal (Pt, Rh, Pd) catalysts containing ceria as support or promoter are very important due to the unique acid–base and redox properties of ceria that can influence (Damyanova and Bueno, 2003):

i. the thermal resistance of the support
ii. the dispersion of supported metals
iii. the oxidation and reduction of supported noble metals
iv. catalytic behavior of metal crystallites
v. the decrease in coke formation on the catalyst surface due to the high oxygen storage capacity (OSC) of ceria.

The influence of ceria addition to a precious metal (Pt, Pd or Rh)/Al_2O_3 catalyst on the mechanism for the CO oxidation has been studied by several authors. Except for large oxygen-excess atmospheres, the addition of ceria lowers the overall activation energy, i.e. increases the activity, reduces the inhibition effect of CO, and makes the oxygen partial pressure dependence less pronounced. From these observations, the participation of oxygen originating from ceria in the reaction was proposed. This reaction of ceria–oxygen with CO

is also believed to be responsible for the observed CO_2 desorption in temperature-programmed desorption, after CO adsorption on Pt/CeO_2 (Holmgren *et al.,* 1999).

Ceria enhances the reactivity of Pt when it is prereduced. The presence of ceria together with Pt seems to lead to new very reactive sites on $Pt\text{-}CeO_2/Al_2O_3$. The reaction on $Pt\text{-}CeO_2/Al_2O_3$ may consist of the formation of CO_2 via the reduction of the interfacial ceria by CO adsorbed on Pt and a noncompetitive Langmuir–Hinshelwood mechanism can be imagined on the metal/oxide interface. The CO_2 desorption leads to vacant sites on the interfacial Pt and makes the dissociative adsorption of gaseous oxygen possible. Ceria is then regenerated by a spillover phenomenon of O_{ads} (on the Pt sites of the $Pt\text{-}CeO_2$ interface) toward Ce_2O_3 and reoxidation of the interface into CeO_2. This interpretation is described by three consecutive steps as shown below (Serre *et al.*, 1993).

$$CO_{ads} + 2\ CeO_2 \longrightarrow CO_2 + * + Ce_2O_3 \quad (2.7)$$

$$½\ O_2 + * \longrightarrow O_{ads} \quad (2.8)$$

$$O_{ads} + Ce_2O_3 \longrightarrow 2\ CeO_2 + * \quad (2.9)$$

Özkara and Aksoylu (2003) reported that ceria can be an adequate support for Pt when one has to lower the CO concentration in a hydrogen-rich stream by using the PROX reaction at low temperature and/or with a minimum hydrogen loss. Unfortunately, ceria-supported platinum was found to be too active in hydrogen oxidation as well, and cannot be considered as an effective PROX catalyst above 130 ºC. Nevertheless, ceria can be considered as a beneficial additive to supported Pt catalysts (Wootsch *et al.*, 2004).

2.3.3. Cobalt Oxide (CoO_x) Promoters

Metal-containing supported systems are widely studied as catalysts for a number of heterogeneous processes, and not only for platinum group metals but also for 3*d* metals (Co, Cu, Mn, etc.). Study of such systems in the environmentally important reaction of CO oxidation is needed both from the practical and the theoretical viewpoint (Oleksenko, 2004). Cobalt oxides are one of the versatile materials among the transition metal oxides. It has been reported that unsupported cobalt oxide is an active catalyst in air pollution control for CO oxidation, NO reduction by some hydrocarbons, NO decomposition, and abatement

of organic pollutants from effluent streams. Also, cobalt oxides are important in the Fischer-Tropsch synthesis, development of the rechargeable battery and the CO sensor (Lin *et al.,* 2003).

On the last decade, several new cobalt-based catalysts promoted by small amounts of noble metals are reported to be very effective for car exhaust purification or other catalytic reactions. These studies have indicated that the presence of a small amount of noble metals has greatly enhanced the activity of the cobalt-based catalysts (Meng *et al.,* 1997).

It is known that Co_3O_4 and CoO are the stable oxides in the cobalt oxide system, while the valence of cobalt higher than +3 is thermally unstable (Lin *et al.,* 2003). El-Shobaky and Deraz (2001) reported that cobaltic oxide (Co_3O_4) belongs to a p-type semiconductor group and has a spinel structure. Co_3O_4 is stable at temperatures below 800 °C, above which it decomposes readily forming CoO which interacts with atmospheric oxygen giving cobaltic oxide. Cobalt oxides exhibit high catalytic activities in CO oxidation.

Cobalt oxides are known for having high activity for CO oxidation even at temperatures below 220 K under dry conditions. It was shown that pre-oxidation of cobalt oxide yields a highly active surface for CO oxidation and Co_3O_4/Al_2O_3 has high CO oxidation activity even without the presence of noble metals. CO seems to be unable to block the cobalt oxide surface from O_2 adsorption as it does on platinum. But the cobalt oxide is slowly deactivated during CO oxidation, and the presence of water and hydrocarbons reduce the activity of the preoxidized cobalt oxide significantly (Thormählen *et al.,* 1999).

Epling *et al.* (2003) proposed that the supported Co catalyst is as active as the Pt catalyst at high temperatures. However, at low temperatures, it is inactive for CO oxidation, probably due to its water sensitivity. Based on activity, Co could be a good replacement for Pt at operating temperatures above 120 °C. However, it is inhibited by the other reformate gases, H_2O and CO_2.

Yan *et al.* (2004) stated that CoO_x could serve as O-supplier. Cobalt ion may also promote the adsorption of O_2 on Pt by an increased electron back donation into the anti-bonding orbital of molecularly adsorbed O_2. They also stated that the co-existence of H_2O and CO_2 in the feed showed a positive net effect on both conversion and selectivity at temperatures below 120 °C for PROX reaction.

Törncrona *et al*. (1997) studied CO oxidation over palladium or platinum supported on alumina. By promoting Pd with cobalt oxide, the activity for oxidation of carbon monoxide significantly increased. The oxidation of CO started about 100 °C lower over cobalt oxide promoted Pd compared with unpromoted Pd.

The promoting effect of cobalt oxide on Pt may be understood as follows: At about 100 °C, CO starts to desorb from the cobalt sites. This leaves free sites for oxygen adsorption and subsequent reaction between CO and O. When the oxygen atoms are present close to the interface between Pt and Co, the reaction may spillover to Pt where a more rapid light-off, compared with Co, can take place, and the oxygen reacts with CO adsorbed on Pt. This, in turn, gives free sites for oxygen adsorption on Pt followed by oxidation of CO (Törncrona *et al*., 1997).

Disadvantages of cobalt oxide, at high temperatures and in the presence of water, are sintering of the active phase and reaction with alumina supports, leading to formation of the fairly inactive spinel $CoAl_2O_4$ (Törncrona *et al*., 1997).

2.3.4. Aluminum Oxide (Al_2O_3) Support

A support can be described as an inert substance that provides a means of spreading out an expensive catalyst ingredient such as platinum for its most effective use, or a means of improving the mechanical strength of an inherently weak (metal/active phase) catalyst. However, the support may actually contribute to catalytic activity, depending upon the reaction type and conditions, and it may react to some extent with other catalyst ingredients during the manufacturing process (Satterfield, 1991). The selection of a support is based on its desirable characteristics, such as the followings:

- A support must have desirable mechanical properties including attrition resistance, hardness, and comparative strength.
- It should be stable under reaction and regeneration conditions.
- It should provide surface area enough to guarantee targeted dispersion of active phases. High surface area is usually, but not always, desirable.
- The support must supply porosity, including average pore size and pore-size distribution. High area implies fine pores, but relatively small pores may become plugged in catalyst preparation, especially if high loadings are sought.
- It should have low cost.
- It should be inert or provide active sites for activity or strong metal/support interaction depending on the reaction.

Of a wide range of possible supports, only three materials combine these characteristics optimally, and they account for most industrial supported catalysts: alumina, silica, and carbon (mainly activated carbon) (Özkara, 2002).

γ-Al_2O_3 is considered as the most convenient support for a big variety of catalysts especially those used in oxidation and reduction reactions. However, the catalytic activities of γ-Al_2O_3-supported solids decrease progressively as a function of time of use due to an enhanced formation of metal aluminate which exhibits a lower catalytic activity as compared with the metal oxide itself (El-Shobaky *et al*., 1998).

It was reported that the reaction between transition metal oxides and Al_2O_3 to produce metal aluminate is strongly dependent upon the nature of the transition metal element. The rate of reaction between the metal oxide and Al_2O_3 decreases in the following order: Cu>Co>Ni>>Fe (El-Shobaky *et al*., 1998).

Wang *et al*. (2003) stated that Al_2O_3 is not regarded as a good support for gold catalysts. Schubert *et al*. (2001) showed that Al_2O_3 was very different from reducible oxides such as FeO_x, NiO_x, and CoO_x. When gold is supported on Al_2O_3, which is believed to behave as neutral in the reaction process, only moderately active catalysts are obtained. Therefore, gold catalysts supported on composite MO_x/Al_2O_3 seem to have the possibility

to realize the commercialization of high-activity catalysts. It is desirable to develop this kind of $Au/MO_x/Al_2O_3$ catalysts for practicable applications (Wang *et al*., 2003).

Hightower *et al.* (1976) reported that precious metal catalysts such as platinum and palladium exhibit a capable light-off characteristic for CO oxidation, whereas base metal catalysts such as γ-Al_2O_3 supported copper oxides have poorer behavior in this aspect. A comparison of the catalytic activities of Cu/SDC and Cu/SDC/γ-Al_2O_3 catalysts reveals that catalysts supported on γ-Al_2O_3 exhibit lower activities, although they possess much higher surface areas (Wang *et al*., 2000).

Schubert *et al*. (1997) stated that over Pt/Al_2O_3 during CO oxidation in a hydrogen-rich mixture, DRIFTS measurements revealed the presence of surface formate species which were formed at the metal/support interface and strongly enhanced by the water in the gas phase or the water formed from the hydrogen oxidation. If the hydration of the support is the main cause of the enhancement, the effect of water partial pressure would be manifested only in the very low partial pressure region, but addition of water to the dry feed mixture did not affect the CO conversion. It seems that the small amount of water formed by the side reaction, hydrogen oxidation, was sufficient to hydrate the support (Kim and Lim, 2002).

Generally, platinum is known to be a poor catalyst for methanation reactions when compared to Ni or Ru. Demmin and Gorte (1987) reported that the methanation reaction in H_2/CO mixtures, occurring at a very low rate on polycrystalline Pt under atmospheric pressure, can be enhanced if Pt is supported on oxide materials. This support-induced enhancement decreases in the order of TiO_2>Al_2O_3>SiO_2 (Kachlich *et al*., 1997).

Hasegewa *et al*. (2002) reported that the γ-Al_2O_3 has a large surface area and is also used as a supporting material for catalysts. If a H_2-selective silica membrane is combined with a γ-Al_2O_3 film which is loaded with a noble metal catalyst, the CO concentration can be decreased to levels below the threshold value.

2.4. Reaction Mechanisms for CO Oxidation

Catalysis and kinetics are still very important in homogeneous and heterogeneous reactions for industrial applications. Although most industrial processes were resolved during the past century, there are space for new developments of catalysts and processes in environment, fuel cells, natural gas conversion, new materials and nowadays in biotechnology. The main questions arising from industrial point of view are the stability and selectivity. From the scientific point of view, it urges to questions concerning the understanding of the reaction mechanism and the kinetics (Schmal *et al.,* 2005).

The foregoing concerns are for kinetic modeling on the basis of elementary steps, because such models have a larger impact. An even more important advantage of elementary step modeling is that a model can be determined experimentally for one global reaction, but applied in a combination of elementary step kinetics for other global reactions. In this way, mutual interactions between different global reactions, as may happen because of common gas phase or surface species, can be simply accounted for (Hoebink *et al.,* 2001).

Kinetic modeling on the basis of elementary steps exploits the law of mass action, which is the best possible rate equation. It is sometimes argued that elementary step kinetics contain too many parameters that impedes making of any description about experimental data. It should be realized, however, that each step preferably is proven relevant on the basis of experimental evidence, and quite often such relevance has already been reported in the literature from studies that applied completely different techniques. Moreover, the rate parameters should have significant values from a statistical point of view, as to be obtained from multiresponse nonlinear regression, and these values should be consistent with well-established theories. Modeling via elementary steps also allows to adapt the kinetic model when the catalyst formulation is changed in order to introduce new catalytic functions (Hoebink *et al.,* 2001).

A lot of studies on catalytic oxidation of carbon monoxide under dynamic conditions refer to the reaction proceeding over supported noble metal catalysts. The number of studies regarding CO oxidation over oxide catalysts is substantially lower. Even less is the

number of studies that include elementary-step modeling of the diffusion of subsurface lattice oxygen in carbon monoxide oxidation over oxide catalysts (Sedmak *et al.,* 2004).

The detailed mechanism of the simultaneous oxidation of CO and H_2 over noble metals is not yet fully understood. H_2 oxidation is strongly inhibited by the presence of CO, because CO chemisorption on noble metal surfaces is much stronger than H_2 or O_2 chemisorption. Consequently, CO blankets the metal surface, displacing the weakly chemisorbed H_2 and O_2 species, and prevents reaction unless the temperature is high enough to desorb some of the CO on the surface. This indicates that the light-off behavior of noble metals in CO–H_2–O_2 mixtures is dominated by the kinetics of CO oxidation rather than by the kinetics of H_2 oxidation. Alternatively, the H_2 in the feed can interact with CO chemisorbed on the surface to form a complex such as H–CO; its easier desorption from the surface may increase the CO oxidation activity significantly (Trimm and Önsan, 2001).

There seems to be general consensus on most of the elementary steps constituting the reaction mechanism of the CO oxidation by O_2 over group VIII metals which has been studied extensively during the past decades. CO chemisorption on noble metals is generally considered to proceed molecularly via a precursor state. Oxygen adsorption was found to proceed dissociatively at temperatures above 100 K, however, molecularly adsorbed oxygen is often included in reaction mechanisms. This is substantiated physically by assuming that molecular chemisorption of oxygen is followed by potentially faster dissociation. Significant associative desorption of oxygen adatoms has not been observed at temperatures lower than 700 K (Nibbelke *et al.,* 1997).

Nibbelke *et al.* (1998) developed a transient kinetic model based on elementary reaction steps for the CO oxidation by O_2 in the absence of H_2O and CO_2 over a Pt/Rh/CeO_2/Al_2O_3 three-way catalyst. The model incorporates both the monofunctional and bifunctional paths. "*" represents the Pt sites and "s" represents the ceria sites in Table 2.1.

Jansson *et al.* (2001) proposed a model for low temperature CO oxidation on cobalt oxide based on flow reactor studies, isotope experiments and in situ FTIR studies as below:

i. CO adsorbs on the cobalt oxide surface.

ii. The adsorbed CO reacts with activated oxygen, already present on the cobalt oxide surface and desorbs as CO_2. A carbonate species might be formed as an intermediate.

iii. The reduced cobalt is reoxidized by gas phase oxygen or it is further reduced by CO thus deactivating the site.

iv. CO_2 can adsorb on the surface and form surface carbonate species.

Table 2.1. Elementary step reaction path considered for kinetic modeling of the oxidation of CO by O_2 in the absence of H_2O and CO_2 over a $Pt/Rh/CeO_2/Al_2O_3$ catalyst (Nibbelke *et al.,* 1998)

	Reaction Path			
Elementary Step	A	B	C	Step Number
	[a]σ_A	σ_B	σ_C	
$CO + * \underset{k_1^b}{\overset{k_1^f}{\Leftrightarrow}} CO*$	2	0	2	(1)
$O_2 + * \overset{k_2^f}{\rightarrow} O_2*$	1	1	0	(2)
$O_2* + * \overset{k_3^f}{\rightarrow} 2O*$	1	1	0	(3)
$CO* + O* \overset{k_4^f}{\rightarrow} CO_2 + 2*$	2	0	0	(4)
$CO + O* \underset{k_5^b}{\overset{k_5^f}{\Leftrightarrow}} OCO*$	0	2	0	(5)
$OCO* \overset{k_6^f}{\rightarrow} CO_2 + *$	0	2	0	(6)
$O_2 + s \overset{k_7^f}{\rightarrow} O_2s$	0	0	1	(7)
$O_2s + s \overset{k_8^f}{\rightarrow} 2Os$	0	0	1	(8)
$CO* + Os \overset{k_9^f}{\rightarrow} CO_2 + * + s$	0	0	2	(9)
$CO_2 + \gamma \underset{k_{10}^b}{\overset{k_{10}^f}{\Leftrightarrow}} CO_2\gamma$	0	0	0	(10)
$2CO + O_2 \rightarrow 2CO_2$				

[a]Stoichiometric coefficients for elementary steps of path *i* (σ_i)

Epling *et al.* (2003) proposed a possible mechanism for $Pt\text{-}Co/TiO_2$ in which the platinum causes a further reduction in neighboring cobalt sites which adsorb more of the O_2 and lend this reactant to the CO adsorption sites, most likely associated with the Pt. Pt

readily adsorbs CO but does not readily adsorb O_2 at these low temperatures. Since O_2 is never found in the effluent, it must be chemisorbed on some part of the catalyst. Therefore, this limiting step may be partially overcome by the presence of the more reduced Co species at the surface.

Nibbelke *et al.* (1997) developed a steady state kinetic model based on elementary reaction steps for the CO oxidation by O_2 in the presence of H_2O and CO_2 over a $Pt/Rh/CeO_2/Al_2O_3$ three-way catalyst. The model incorporates both the monofunctional and bifunctional paths. "*" represents the Pt sites and "s" represents the ceria sites as shown below in Table 2.2.

Table 2.2. Elementary step reaction path considered for kinetic modeling of the oxidation of CO by O_2 in the presence of H_2O and CO_2 over a $Pt/Rh/CeO_2/Al_2O_3$ catalyst (Nibbelke *et al.,* 1997)

	Reaction Path			
Elementary Step	A	B	C	Step Number
	[a]σ_A	σ_B	σ_C	
$CO + * \underset{k_1^b}{\overset{k_1^f}{\Leftrightarrow}} CO*$	2	2	2	(1)
$O_2 + 2s \overset{k_2^f}{\rightarrow} 2Os$	1	1	1	(2)
$2Os \overset{k_3^f}{\rightarrow} O_2 + 2s$	0	1	0	(3)
$O_2 + s \overset{k_4^f}{\rightarrow} O_2s$	0	0	1	(4)
$O_2s + s \overset{k_5^f}{\rightarrow} 2Os$	0	0	1	(5)
$CO* + Os \overset{k_6^f}{\rightarrow} CO_2 + * + s$	2	2	2	(6)
$2CO + O_2 \rightarrow 2CO_2$				

Rajasree *et al.* (2004) investigated the applicability of the dynamic model developed by Nibbelke *et al.* (1998) for a Pd-loaded ceria-zirconia mixed oxide catalyst and extended for CO oxidation by O_2 in the presence of H_2O and CO_2. Their study shows that this model can be applied for simulating the transient behavior over other three-way catalysts. They

also proposed an alternative elementary step reaction path considered for kinetic modeling of the effect of water on the oxidation of CO by O_2. "*" represents the Pd sites and "s" represents the ceria sites in Table 2.3.

Table 2.3. Elementary step reaction path considered for kinetic modeling of the effect of water on the oxidation of CO by O_2 over a Pd-loaded ceria-zirconia mixed oxide catalyst (Rajasree *et al.,* 2004)

	Reaction Path	
Elementary Step	A	Step Number
	$^{a}\sigma_A$	
$CO + * \underset{k_1^b}{\overset{k_1^f}{\Leftrightarrow}} CO*$	2	(1)
$O_2 + s \overset{k_4^f}{\rightarrow} O_2s$	1	(2)
$O_2s + s \overset{k_5^f}{\rightarrow} 2Os$	0	(3)
$H_2O + s \underset{k_4^b}{\overset{k_4^f}{\Leftrightarrow}} H_2Os$	0	(4)
$H_2Os + Os \underset{k_5^b}{\overset{k_5^f}{\Leftrightarrow}} 2OHs$	1	(5)
$CO* + OHs \overset{k_6^f}{\rightarrow} CO_2 + Hs + *$	2	(6)
$2Hs + Os \overset{k_7^f}{\rightarrow} H_2Os + 2s$	1	(7)
$2CO* + 2Os \rightarrow 2CO_2 + 2* + 2s$		

2.5. Methods for Kinetic Analysis

Kinetic experiments on heterogeneous catalytic reactions are generally carried out in plug flow reactors. To keep the interpretation as simple as possible, the flow is considered to be perfectly ordered with uniform velocity. This requires a sufficiently high velocity and a tube-to-particle diameter ratio of at least 10, to avoid too much short-circuiting along the wall, where the void fraction is higher than in the core of the bed. The tube diameter should not be too large either, however, to avoid radial gradients of temperature and

concentration, which again lead to complications in the interpretation. For this reason, temperature gradients in the longitudinal, i.e. in the flow direction, should also be avoided.

Although computers can handle nonisothermal situations up to a certain extent, determining the functional form of the rate equation is possible only on the basis of isothermal data. Care should be taken to minimize heat transfer resistance at the outside and inside walls. If isothermicity is still not achieved, the only remaining possibility is to dilute the catalyst bed. Excessive dilution has to be avoided as well, because all the fluid streamlines should hit the same number of catalyst particles (Froment and Bischoff, 1990).

The starting point for evaluating the rate of reaction in an ideal plug flow reactor is Equation (2.10), or at steady state, Equation (2.11) (Fogler, 1992).

$$\begin{bmatrix} Flow \\ rate \\ in \end{bmatrix} - \begin{bmatrix} Flow \\ rate \\ out \end{bmatrix} + \begin{bmatrix} Rate\ of \\ generation \end{bmatrix} = \begin{bmatrix} Rate\ of \\ accumulation \end{bmatrix} \tag{2.10}$$

$$F_{Ao} - F_{Ae} + (r_A)(W) = 0 \tag{2.11}$$

It is usually better to start with an integral method when it is needed to determine kinetics for a new system. The integral method gives an approximate rate equation with a quick and easy experiment. Differential method is required only when a precise rate equation is needed. If 10 per cent change in rate matters, differential rate measurements are necessary. Differential measurements take 10-100 times longer than integral measurements, so differential methods are useful only when a high degree of accuracy is needed (Masel, 2001).

2.5.1. The Differential Method of Kinetic Analysis

Kinetic studies designed to identify reaction mechanisms are often aimed at the mechanism in the initial stages of a forward reaction, before any complications due to reverse reactions or inhibition by products can appear. The study of such conditions

involves observing small changes in conversion starting from pure reactants, i.e. from zero conversion.

In principle, plug flow reactors can be operated in a differential mode at any level of conversion by incrementing the space time between composition readings and observing the small increments in conversion that results. However, the use of plug flow reactors in the differential mode at low levels of conversion presents significant problems. In the case of a plug flow reactor operating at low conversion, high pressure drop due to the required high flow rates can be an obstacle. Higher levels of conversion serve no special purpose for differential method (Wojciechowski and Rice, 2003). Masel (2001) reported the advantages and disadvantages of differential method as in Table 2.4.

Table 2.4. Advantages and disadvantages of the differential method of kinetic analysis (Masel, 2001)

Advantages	Disadvantages
Get rate equation directly	Difficult experiment
Easy to fit data to a rate law	Need many runs
High confidence on final rate equation	Not suitable for very fast and very slow reactions

In the case of a plug flow operating in a differential way, the amount of catalyst is relatively small so that the conversion is limited and may be considered to occur at a nearly constant concentration of A. The continuity equation for A then takes the form below and r_A follows directly from the measured conversion. Very accurate analytical methods are required in this case. Furthermore, it is always a matter of debate how small the conversion has to be to fulfill the requirements (Froment and Bischoff, 1990).

$$F_{Ao}\,\Delta X_A = r_A\,\Delta W \tag{2.12}$$

Normally, the objective is to determine the kinetics of the reaction from experimental data. To accomplish this objective in a plug flow reactor, many runs would be made, each with a different feed composition but at the same temperature. Then various forms of the

rate equation would be compared with the experimentally determined rates as functions of reactant concentrations to establish the best rate expression using a regression method. Subsequent runs at different temperatures could be made to establish the activation energy (Smith, 1981).

Although the result is a straightforward analysis of rate data, there are a few pitfalls in analyzing the rate data via a differential method (Masel, 2001):

- It is not uncommon for more than one rate equation to fit the measured kinetics within the experimental uncertainties. One should not infer that the rate equation is correct just because the data fits.
- The quality of kinetic data varies with the equipment used and the method of temperature measurement and control. Data taken on one apparatus are seldom directly comparable to data taken on a different apparatus.
- It is not uncommon to observe 10-30 per cent variations in rate taken in the same apparatus on different days. Usually, these variations can be traced to variations in the temperature, pressure, or flow rate in the reactor.
- The procedure used to fit the data can have a major effect on the values of the parameters obtained in the data analysis.
- The quality of the regression coefficient (R^2) does not tell you how well a model fits your data.

2.5.2. The Integral Method of Kinetic Analysis

When the conditions of approximately constant rate cannot be met in a once-through reactor, the measured conversion data will represent the integrated value of the rates in all parts of the reactor. A laboratory unit operated in this way is termed an integral reactor.

A complete set of integral reactor data consists of measurements of the conversion for different flow rates through the reactor, with each run made at constant reactants ratio, pressure and temperature (if possible). Then an additional set of conversion vs. flow runs is made at a different reactants ratio but the same pressure and temperature. This procedure is continued until data are obtained over the entire range of reactants ratio and temperature. A

useful means of summarizing the results is to prepare graphs of W/F vs. conversion at constant values of reactants ratio and P_t. Such graphs for representing the experimental data are suggested by the integrated form of the continuity equation for A in terms of conversion (Equation 2.13). The shape of these curves is determined by the nature of the rate, and they provide some qualitative information about the rate equation (Smith, 1981).

$$\frac{W}{F_{A_o}} = \int_{x_{A1}}^{x_{A2}} \frac{dx_A}{r_A} \tag{2.13}$$

In the integral method, a rate equation is assumed and then the plug flow design expression is integrated for the reactor flow conditions. This integration gives a relationship between W/F and conversion which may be compared with the experimental data. The final step is the choice of the rate equation that gives the best agreement with the experimental W/F vs. conversion curves for all conditions of reactants ratio, temperature and pressure (Smith, 1981).

Masel (2001) reported the advantages and disadvantages of integral method as in Table 2.5.

Table 2.5. Advantages and disadvantages of the integral method of kinetic analysis (Masel, 2001)

Advantages	Disadvantages
Easier experiment	Must infer rate equation
Can do a few runs and get important information	Hard to analyze rate data
Suitable for all reactions including very fast or very slow ones	Low confidence on final rate equation

3. EXPERIMENTAL WORK

3.1. Materials

3.1.1. Chemicals

The chemicals used for catalyst preparation are listed in Table 3.1.

Table 3.1. Chemicals used in catalyst preparation

Chemicals	Formula	Grade	Source	Molecular Weight (g/mole)
Tetraammineplatinum (II) nitrate	$Pt(NH_3)_4(NO_3)_2$	Research	Aldrich	387.21
Cobalt Nitrate hexahydrate	$Co(NO_3)_2.6H_2O$	Extra Pure	Merck	291.04
Cerium(III) nitrate hexahydrate	$Ce(NO_3)_2.6H_2O$	Extra Pure	Merck	434.23
Aluminium Oxide	Al_2O_3	Extra Pure	Zeochm EU	101.96

3.1.2. Gases and Liquids

The liquids and gases used in this study were listed with their applications and specifications in the Tables 3.2 and 3.3. All of the gases used in this study were supplied by BOS and HABAŞ Companies, Istanbul, Turkey**.**

Table 3.2. Applications and specifications of the gases used

Gas	Application	Specification
Carbon monoxide	Reactant, GC calibration	99.0% HABAŞ
Oxygen	Reactant, GC calibration	99.99% BOS
Carbon dioxide	Reactant	99.99% BOS
Hydrogen	Reactant, Reducing agent	99.99% BOS
Helium	Reactant (Inert)	99.99% BOS
Helium	GC Carrier	99.99% BOS

Table 3.3. Applications and specifications of the liquids used

Liquid	Application	Specification
Water	Reactant, cleaning	Distilled

3.2. Experimental Setup

The experimental systems used may be described in three groups:

- Catalyst preparation system; used for catalyst preparation by impregnation
- Microreactor flow system; consists of tubing, the controller box, reactor, furnace, temperature controller, water pump, heating line to vaporize water, cold trap, gas chromatograph and data processor
- Product analysis system; is connected to the microreactor flow system. It consists of a gas sampling section, a gas chromatograph and a data processor.

3.2.1. Catalyst Preparation System

Catalysts were prepared by impregnation method using the system presented in Figure 3.1. The support placed in vacuum flask was impregnated with an aqueous solution of precursor. Precursor solution was prepared in the beaker and pumped by the peristaltic pump through the silicone tubing.

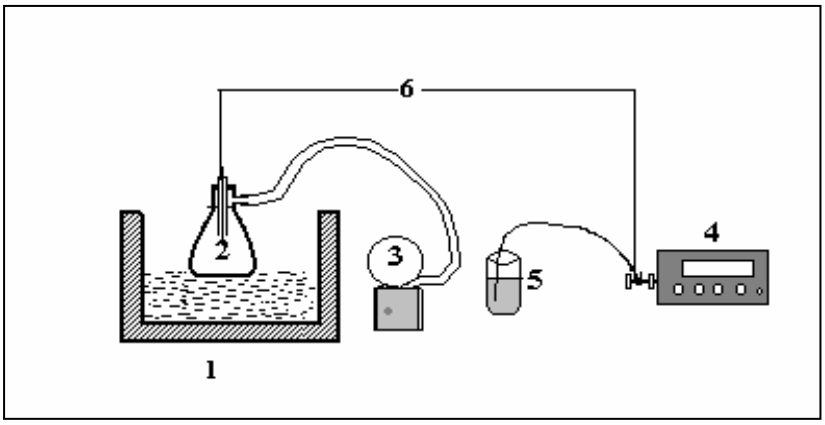

Figure 3.1. The impregnation system: 1. Ultrasonic mixer 2. Vacuum flask 3. Vacuum pump 4. Peristaltic pump 5. Beaker 6. Silicone tubing

3.2.2. Microreactor Flow System

1/4" and 1/8" o.d. stainless steel and copper tubing-fittings and research grades of all pure CO, CO_2, O_2, H_2 and He gases were used. Their flow rates were controlled using four Brooks 5850E mass flow controllers and one Aalborg 4PROC mass flow controller. The water was pumped into the preheated (150 ºC) reactant gas mixture using a Jasco PU-2080Plus HPLC pump, and evaporated in a glass wool bed before reaching the catalyst.

All gases were mixed before they entered the reactor. The feed mixture was allowed to flow through 50cm long - 4 mm i.d. stainless steel fixed bed down-flow reactor containing required amount of catalyst. The reactor was put inside the furnace that heated the reactor to the desired temperature. The spaces between inlet of the reactor-furnace and the outlet of the reactor-furnace were closed by ceramic wool to prevent heat loss and maintain stable temperature profile. The catalyst sample was placed in the middle of the reactor tube above a bed support made by squeezing the silane treated glass-wool (Alltech Associates Inc.).

The temperature of the catalyst bed was controlled by Shimaden FP-21 controller in a 40 cm X 2.4 cm i.d. tube furnace. The K-type sheathed thermocouple is placed at the midst of the catalyst outside the microreactor.

3.2.3. Product Analysis System

Product streams were analyzed using a Shimadzu GC-8A gas chromatograph connected to a Shimadzu CR-4A data processor. Molecular Sieve 5A (60-80 mesh) column and a TCD were used in analysis. The excess water could harm the chromatograph column so a cold trap was placed in the tubing line just before the gas flow reached the chromatograph in order to condense the water. Cold trap consisted of an ice box and coiled tubing to increase contact time of flow through a cold environment.

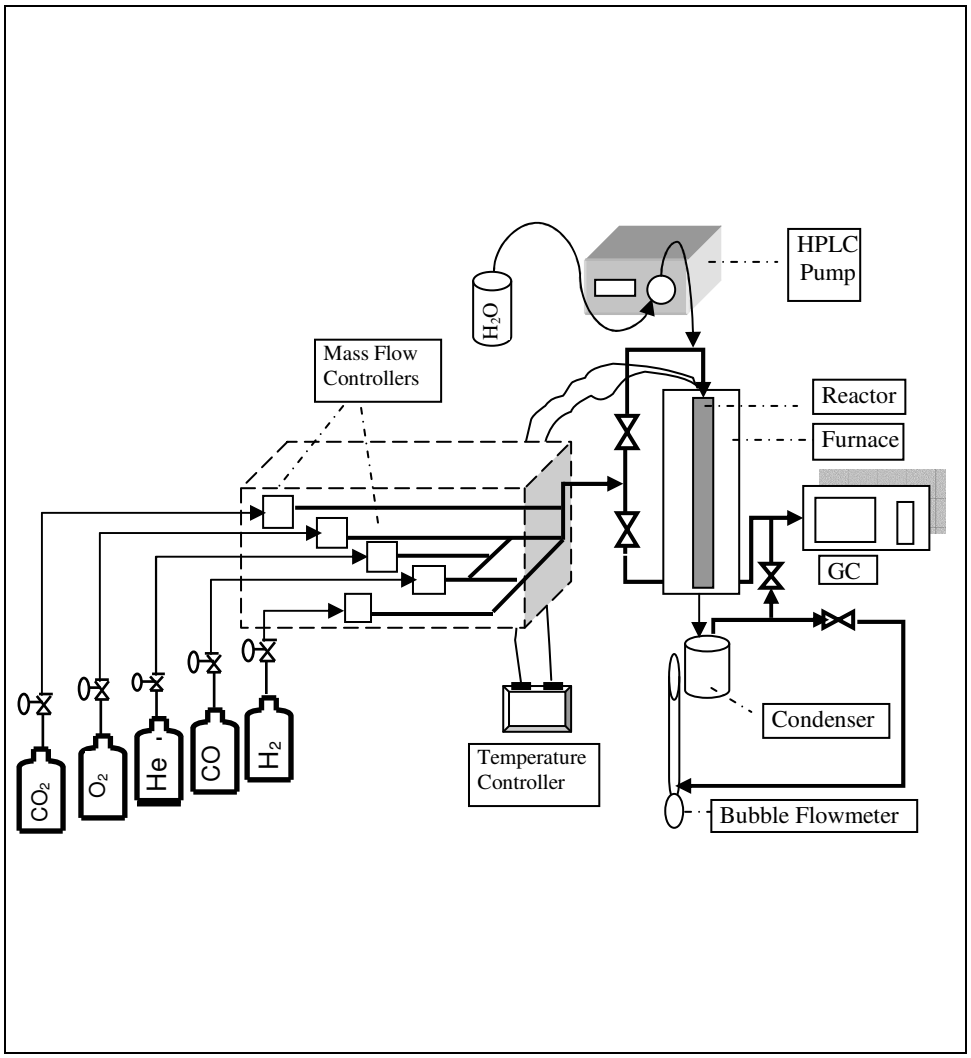

Figure 3.2. The microreactor flow and product analysis system

3.3. Catalyst Preparation

The catalyst was prepared by incipient to wetness impregnation. It contained 1.4 weight per cent Pt, 1.25 weight per cent Ce and 1.25 weight per cent Co. The experimental setup shown in Figure 3.1 was used for catalyst preparation. The procedure had four parts:

i. Evacuating the support
ii. Contacting the support with the precursor solution
iii. Drying
iv. Calcination.

Alumina support was crushed and sieved into 45-60 mesh size (344 -255 μm). It was calcined at 450 ºC for 5 hours prior to impregnation. Five grams of support was placed in a vacuum flask and kept under vacuum for 30 min. Thus, trapped air in pores of the support that could prevent penetration of the precursor solution was eliminated. This was accompanied by mixing in an ultrasonic mixer.

All the metal salts were dissolved in 1.21 ml of water per gram of alumina support. Aqueous precursor solution was fed to the vacuum flask at a flow rate of 0.5 ml/min via silicone tubing. A Masterflex computerized-drive peristaltic pump was used to feed the solution. The slurry was mixed under vacuum by an ultrasound mixer to maintain uniformity of impregnation. Impregnated support was mixed for additional 90 min. The slurry obtained was dried at 115 ^{o}C overnight (16 hours). The catalyst was then calcined at 450 ºC for 2 hours.

3.4. Kinetic Measurements

All catalysts were reduced in situ by H_2 before the reaction took place and kept under He flow until the reaction test was performed. The reduction program can be seen for the catalyst in the following Table 3.4.

Table 3.4. Reduction program for Pt-Co-Ce/Al_2O_3 catalyst

Segments	Starting and End Temperatures	Segment Gas
First Segment	Heating from 25 ºC to 375 ºC with a heating rate 2.5 ºC/min	He with flow rate of 50 ml/min
Second Segment (Reduction)	Keeping constant at 375 ºC for 3h	H_2 with flow rate of 50 ml/min
Third Segment	Flushing at 375 ºC for 1h to clean the catalyst surface	He with flow rate of 50 ml/min
Fourth Segment	Overnight cooling down to 25 ºC	He with flow rate of 25 ml/min

In order to keep conversions at low values, small amounts of catalyst, i.e. 10 mg or 20 mg, were put into the reactor. To minimize axial dispersion, the catalyst bed was diluted using inert γ-Al_2O_3 such that the total bed weight remained constant at 250 mg. Total flow rate was kept at 100 ml/min for all reactions and 45-60 mesh size (344-255 μm) particle size was selected. These conditions were determined to be sufficient for the elimination of the external and internal transport resistances, respectively (İnce, 2004; Uysal, 2005). The reaction conditions for the catalyst in the presence of 25 per cent CO_2 and 10 per cent H_2O, and in the absence of CO_2 and H_2O are given in Tables 3.5 and 3.6, respectively.

Besides all kinetic experiments, a blank test was also conducted to ensure that the material of construction, glass-wool and γ-alumina (used as inert material within the catalyst bed) did not interfere with the reaction test results. The items above were found to be inactive under the conditions used in the kinetic experiments. Kahlich *et al.* (1997) were also reported that with pure γ-Al_2O_3, the conversion of both O_2 and CO is well below 0.5 per cent of their total amounts over the entire temperature range investigated in the differential flow mode ($\leq$250 °C).

Table 3.5. The reaction conditions studied with Pt-Co-Ce/Al_2O_3 catalyst in the presence of 25% CO_2 and 10% H_2O

T_{rxn} (ºC)	Total Flow (ml / min)	Weight of Catalyst (mg)	Feed Composition (%) with He as Balance				
			H_2	O_2	CO	CO_2	H_2O
110	100	10	60	0.5	1	25	10
110	100	20	60	0.5	1	25	10
110	100	10	60	0.75	1	25	10
110	100	20	60	0.75	1	25	10
110	100	10	60	1	1	25	10
110	100	20	60	1	1	25	10
110	100	10	60	1.25	1	25	10
110	100	20	60	1.25	1	25	10
110	100	10	60	1.5	1	25	10
110	100	20	60	1.5	1	25	10
110	100	10	60	1	0.5	25	10
110	100	20	60	1	0.5	25	10
110	100	10	60	1	0.75	25	10
110	100	20	60	1	0.75	25	10
110	100	10	60	1	1.25	25	10
110	100	20	60	1	1.25	25	10
110	100	10	60	1	1.5	25	10
110	100	20	60	1	1.5	25	10
120	100	10	60	0.5	1	25	10
120	100	20	60	0.5	1	25	10
130	100	10	60	0.5	1	25	10
130	100	20	60	0.5	1	25	10

Table 3.6. The reaction conditions studied with Pt-Co-Ce/Al_2O_3 catalyst in the absence of CO_2 and H_2O

T_{rxn} (ºC)	Total Flow (ml / min)	Weight of Catalyst (mg)	Feed Composition (%) with He as Balance				
			H_2	O_2	CO	CO_2	H_2O
110	100	10	60	0.5	1	-	-
110	100	20	60	0.5	1	-	-
110	100	10	60	0.75	1	-	-
110	100	20	60	0.75	1	-	-
110	100	10	60	1	1	-	-
110	100	20	60	1	1	-	-
110	100	10	60	1.25	1	-	-
110	100	20	60	1.25	1	-	-
110	100	10	60	1.5	1	-	-
110	100	20	60	1.5	1	-	-
110	100	10	60	1	0.5	-	-
110	100	20	60	1	0.5	-	-
110	100	10	60	1	0.75	-	-
110	100	20	60	1	0.75	-	-
110	100	10	60	1	1.25	-	-
110	100	20	60	1	1.25	-	-
110	100	10	60	1	1.5	-	-
110	100	20	60	1	1.5	-	-

4. RESULTS AND DISCUSSION

In this work, a steady state kinetic model for the CO oxidation by O_2 in the presence of carbon dioxide and water vapor over the Pt-Co-Ce/γ-Al_2O_3 catalyst was studied. The catalyst was first prepared and optimized by İnce (2004) in the absence of carbon dioxide and water vapor, and the effects of carbon dioxide and water vapor on the selective CO oxidation performance was studied by Uysal (2005).

The conversions for CO oxidation are calculated as follows:

$$\text{CO conversion } (\%) = \frac{[CO]_{in} - [CO]_{out}}{[CO]_{in}} x100 \tag{4.1}$$

The surface coverage concentrations of the considered surface species were evaluated from the corresponding continuity equations, which in the steady state can be represented as below:

$$\sum_{j=1}^{N} v_{i,j} r_{w,j} = 0 \tag{4.2}$$

where j is the number of reaction step, N is the total number of reaction steps considered, $v_{i,j}$ is the stoichiometric coefficient of surface species i in the reaction step j, and $r_{w,j}$ is the reaction rate of reaction step j in $\mu mol\ mg_{CAT}^{-1}\ s^{-1}$. The reaction rates of the elementary reaction steps are calculated via the law of mass action and under the Langmuir assumptions of identical active sites, absence of interactions between adsorbates, and confinement of adsorption to a monolayer. Equation (4.2) forms a set of algebraic equations with the surface coverage concentration of the considered surface species as only unknowns for a given gas phase composition, concentration, and temperature. For the kinetic models discussed in this work, this set of algebraic equations was used to build rate expressions for alternative reaction mechanisms. Subsequently, the CO consumption rates were calculated from the surface coverage concentrations.

4.1. Possible Mechanisms for CO Oxidation

All literature on the selective CO oxidation has been reviewed through the consideration of all plausible elementary reactions constituting the CO oxidation mechanism, and they were listed in Table 4.1, where "*" represents the platinum sites, "◘" represents the cobalt sites, and "●" represents the ceria sites as shown below.

Table 4.1. Plausible elementary reaction steps for the CO oxidation mechanism

Elementary Reaction Steps	Step Number	Elementary Reaction Steps	Step Number
$CO + * \Leftrightarrow CO*$	(1)	$H_2O + ◘ \Leftrightarrow H_2O◘$	(14)
$O_2 + * \rightarrow O_2*$	(2)	$H_2O◘ + O◘ \Leftrightarrow 2OH◘$	(15)
$O_2* + * \rightarrow 2O*$	(3)	$O_2 + ● \rightarrow O_2●$	(16)
$CO + O* \Leftrightarrow OCO*$	(4)	$O_2● + ● \rightarrow 2O●$	(17)
$OCO* \rightarrow CO_2 + *$	(5)	$CO* + O● \rightarrow CO_2 + * + ●$	(18)
$CO* + O* \rightarrow CO_2 + 2*$	(6)	$CO◘ + O● \rightarrow CO_2 + * + ●$	(19)
$CO + ◘ \Leftrightarrow CO◘$	(7)	$H_2 + 2● \Leftrightarrow 2H●$	(20)
$O_2 + ◘ \rightarrow O_2◘$	(8)	$2H◘ + O● \rightarrow H_2O● + 2◘$	(21)
$O_2◘ + ◘ \rightarrow 2O◘$	(9)	$2H● + O● \rightarrow H_2O● + 2●$	(22)
$CO* + O◘ \rightarrow CO_2 + * + ◘$	(10)	$H_2O + ● \Leftrightarrow H_2O●$	(23)
$CO◘ + O◘ \rightarrow CO_2 + 2◘$	(11)	$H_2O● + O● \Leftrightarrow 2OH●$	(24)
$H_2 + 2◘ \Leftrightarrow 2H◘$	(12)	$CO* + OH● \rightarrow CO_2 + H● + *$	(25)
$2H◘ + O◘ \rightarrow H_2O◘ + 2◘$	(13)	$CO◘ + OH● \rightarrow CO_2 + H● + ◘$	(26)

No distinction was made between the cobalt and the ceria sites and both are referred to by a single site, i.e. the "s", in the constructed mechanisms for simplicity in Table 4.2. Also, CO_2, H_2O and H_2 need not be considered explicitly in modeling the CO oxidation over Pt-Co-Ce/Al_2O_3 in the presence of CO_2 and H_2O, as their effect on the reaction rates were assumed to be by means of a change in the rate parameters, but not in the reaction mechanism. It is reported that, for the values of inlet CO_2 and H_2O, i.e. approximately 10 per cent of the feed, the dependence of CO conversion on CO_2 and H_2O is small and partial reaction order in H_2O becomes zero at large H_2O values in the feed (Nibbelke *et al.,* 1997).

Rajasree *et al.* (2004) stated that CO_2 inhibits the CO oxidation by decreasing the oxygen storage capacity (OSC) surface available for oxygen adsorption. This in turn decreases the concentration of adsorbed oxygen on OSC, and hinders the interface reaction between the noble metal and the OSC, and hence, the elementary steps considered in this case are the same as in the absence of CO_2. Kim and Lim (2002) also reported that H_2 do not affect the CO conversion as long as the feed contains more than 10 per cent H_2, and beside H_2, CO_2 and H_2O do not influence the CO oxidation.

Several mechanisms based on the elementary reactions determined in Table 4.1 were constructed and those mechanisms were listed as alternative reaction paths in Table 4.2. The descriptions and the rate expressions for each model with the assumptions used were given below in Sections 4.1.1 to 4.1.6.

4.1.1. Reaction Path A

In monofunctional reaction path A in which all the active sites were assumed to be the same, oxygen adsorption is thought to proceed in two steps in series; first the irreversible molecular chemisorption of O_2, followed by the dissociation of O_2* on the noble metal, i.e. steps (3) and (4) in Table 4.2. Although O_2 adsorption was found to proceed dissociatively at temperatures above 100 K, molecularly adsorbed O_2 is often included in reaction mechanisms (Nibbelke *et al.,* 1997; Manuel *et al.,* 2004). CO_2 formation takes place via a Langmuir-Hinshelwood surface reaction, i.e. step (9). In the case of adsorption equilibrium for CO, the rate expression for reaction path A is simplified to Equation (4.3).

$$-r_{CO} = \frac{(2k_3^f P_{O_2})(K_1 k_4^f k_9^f P_{CO}[S]_0 - K_1 k_3^f k_9^f P_{CO} P_{O_2} - 2k_3^f k_4^f P_{O_2})}{K_1 k_4^f k_9^f P_{CO}(K_1 P_{CO} + 1)} \tag{4.3}$$

4.1.2. Reaction Path B

Reaction path B is also a monofunctional path which takes place via the Eley–Rideal step between adsorbed oxygen and gas phase CO comprising the formation of the OCO* surface species on platinum, step (7) in Table 4.2. The OCO* species can either desorb,

leading to O* on the noble metal surface and CO in the gas phase, or the OCO* species can react to CO_2 (Nibbelke *et al.,* 1998). Assuming that molecular chemisorption of oxygen is rate determining, i.e. $k_4^f >> k_3^f$, the rate expression for reaction path B takes the following form:

$$-r_{CO} = \frac{2k_3^f k_7^f k_8^f P_{CO} P_{O_2} [S]_0}{2k_3^f P_{O_2}(k_7^f + k_8^f) + k_7^f k_8^f P_{CO} + 2k_3^f k_7^f P_{CO} P_{O_2}} \tag{4.4}$$

Table 4.2. Elementary step reaction paths considered in the kinetic modeling of CO oxidation by O_2 over Pt-Co-Ce/Al_2O_3 in the presence of H_2O and CO_2

	Reaction Path					
Elementary Step	A	B	C	D	E	Step Number
	[a]σ_A	σ_B	σ_C	σ_D	σ_E	
$CO + * \underset{k_1^b}{\overset{k_1^f}{\Leftrightarrow}} CO*$	2	0	2	1	4	(1)
$CO + s \underset{k_2^b}{\overset{k_2^f}{\Leftrightarrow}} COs$	0	0	0	1	0	(2)
$O_2 + * \overset{k_3^f}{\rightarrow} O_2*$	1	1	0	0	1	(3)
$O_2* + * \overset{k_4^f}{\rightarrow} 2O*$	1	1	0	0	1	(4)
$O_2 + s \overset{k_5^f}{\rightarrow} O_2s$	0	0	1	1	1	(5)
$O_2s + s \overset{k_6^f}{\rightarrow} 2Os$	0	0	1	1	1	(6)
$CO + O* \underset{k_7^b}{\overset{k_7^f}{\Leftrightarrow}} OCO*$	0	2	0	0	0	(7)
$OCO* \overset{k_8^f}{\rightarrow} CO_2 + *$	0	2	0	0	0	(8)
$CO* + O* \overset{k_9^f}{\rightarrow} CO_2 + 2*$	2	0	0	0	2	(9)
$CO* + Os \overset{k_{10}^f}{\rightarrow} CO_2 + * + s$	0	0	2	1	2	(10)
$COs + Os \overset{k_{11}^f}{\rightarrow} CO_2 + 2s$	0	0	0	1	0	(11)
$2nCO + nO_2 \rightarrow 2nCO_2$						

[a]Stoichiometric coefficients for elementary steps of path *i* (σ_i)

4.1.3. Reaction Path C

Reaction path C is the bifunctional reaction path, involving O_2 adsorption on the OSC cobalt-ceria surface, i.e. steps (5) and (6) in Table 4.2, and a reaction between CO adsorbed on the noble metal surface and oxygen from cobalt-ceria at the noble metal/cobalt-ceria interface, i.e. step (10). The cobalt-ceria sites involved in reaction path C are referred to as OSC, i.e. oxygen storage capacity sites and are denoted by "s", which can be sites on top of the cobalt-ceria lattice, or more likely, oxygen vacancies at the surface of the cobalt-ceria lattice. Oxygen atoms become available for reaction at the noble metal/cobalt-ceria interface either directly by adsorption from the gas phase, via surface diffusion of oxygen adsorbed on the cobalt-ceria surface. Bulk diffusion, which is only observed at high temperatures, e.g. for Rh/ceria above 623 K, does not play any role at low temperatures employed in the present study (Nibbelke *et al.,* 1998). Assuming that the noble metal surface is completely covered with CO, i.e. [COS]>>[S], and O_2 chemisorption is potentially slow as compared to its dissociation implying $k_6^f >> k_5^f$, the rate expression for reaction path C is simplified to Equation (4.5).

$$-r_{CO} = \frac{2k_5^f k_{10}^f P_{O_2} [S]_0 [V]_0}{2k_5^f P_{O_2} + k_{10}^f [S]_0} \tag{4.5}$$

4.1.4. Reaction Path D

Reaction path D is a bifunctional path in which the gas phase CO is adsorbed reversibly on both the noble metal and cobalt-ceria sites, i.e. steps (1) and (2). It is known that considerable amount of CO is adsorbed on cobalt sites over cobalt-containing catalysts (Törncrona *et al.,* 1997; Thormählen *et al.,* 1999). O_2 adsorption is thought to proceed in two consecutive steps on cobalt-ceria sites and CO_2 formation takes place via two Langmuir-Hinshelwood surface reactions; one with the adsorbed CO on the noble metal (Mergler *et al.,* 1997; Bunluesin *et al.,* 1998), and the other with the adsorbed CO on the cobalt-ceria sites (Jansson, 2000). Assuming that CO* is the most abundant reaction intermediate, i.e. [COS]>>[S], and CO adsorption on the cobalt-ceria sites is in equilibrium, and additionally, that O_2 chemisorption is potentially slower than its

dissociation implying $k_6^f >> k_5^f$, the rate expression for reaction path D comes into its final form as below:

$$-r_{CO} = \frac{2k_5^f P_{O_2} [V]_0}{K_2 P_{CO} + 1} \tag{4.6}$$

4.1.5. Reaction Path E

In bifunctional reaction path E, the noble metal adsorbs both CO and oxygen. Oxygen is adsorbed also by the cobalt-ceria sites, i.e. steps (5) and (6) in Table 4.2. CO_2 formation is thought to proceed with two individual Langmuir-Hinshelwood surface reactions; one with the dissociated oxygen on the noble metal, i.e. step (9), and the other with the dissociated oxygen on the cobalt-ceria sites, i.e. step (10). With the assumption of CO adsorption equilibrium on the noble metal, and molecular adsorption of oxygen on the noble metal is rate determining implying k_3^f is too small, and also O_2 chemisorption on cobalt-ceria sites is potentially slower as compared to its dissociation, i.e. $k_6^f >> k_5^f$, the rate expression for reaction path E simplifies to Equation (4.7).

$$-r_{CO} = \frac{2k_3^f P_{O_2} [S]_0}{K_1 P_{CO} + 1} + \frac{K_1 k_{10}^f P_{CO} [S]_0 [V]_0}{K_1 P_{CO} [S]_0 + K_1 P_{CO} + 1} \tag{4.7}$$

4.1.6. Other Suggested Mechanisms

Besides five alternative rate expressions obtained from proposed CO oxidation mechanisms in this work, several other rate expressions from other studies in the literature have been also tested for their fitness with the experimental results from the present study.

Nibbelke *et al.* (1997) proposed three alternative reaction paths for CO oxidation over $Pt/Rh/CeO_2/Al_2O_3$ in the presence of H_2O and CO_2. They could not make a distinction between those paths statistically. In their first path, i.e. Reaction Path A in Table 2.2, the oxygen adsorption on the ceria is assumed to proceed reversibly and dissociatively in a single reaction step. With the assumption that the noble metal surface is completely

covered by CO, the CO_2 production rate of the bifunctional reaction path can be expressed as:

$$r_{CO_2} = k_5^f \left[\frac{4k_2^f P_{O_2} + k_5^f - \sqrt{8k_2^f k_5^f P_{O_2} + \left(k_5^f\right)^2}}{4k_2^f P_{O_2}} \right] \tag{4.8}$$

In their second path, i.e. Reaction Path B in Table 2.2, the oxygen adsorption on the ceria is assumed to proceed reversibly and dissociatively in a single reaction step. With the assumption that the noble metal surface is completely covered by CO, and oxygen adsorption is in equilibrium, the CO_2 production rate of the bifunctional reaction path is simplified to Equation (4.9).

$$r_{CO_2} = \frac{k_5^f \sqrt{K_2 P_{O_2}}}{\sqrt{K_2 P_{O_2}} + 1} \tag{4.9}$$

In their last path, i.e. Reaction Path C in Table 2.2, the oxygen adsorption on the ceria is assumed to proceed in two consecutive steps. In step (4) in Table 2.2, oxygen adsorbs molecularly on a single site, followed by dissociation in step (5). With the assumption that the noble metal surface is completely covered by CO, and that oxygen adsorption is potentially slow as compared to its dissociation, i.e. $k_4^f >> k_3^f$, the CO_2 production rate of the bifunctional reaction path can be expressed as follows:

$$r_{CO_2} = \frac{2k_3^f k_5^f P_{O_2}}{2k_3^f P_{O_2} + k_5^f} \tag{4.10}$$

Akın *et al.* (2001) suggested two alternative reaction paths for CO oxidation over Pt-SnO_2/γ-Al_2O_3 in the absence of CO_2 and H_2O in the feed. On the basis of the kinetic analysis, they found the most plausible mechanism to be CO oxidation at the Pt/SnO_2 interface between adjacently chemisorbed CO and O_2, with the reversible dissociative adsorption of O_2, i.e. step (2) in Table 4.3, being the rate-determining step. The mechanism is given in Table 4.3 in which "*" refers to the Pt sites, and "■" refers to the SnO_2 sites.

The following rate expression is obtained using the concept of the most abundant reactive surface species, and hence, neglecting the surface concentration of oxygen in the adsorption term.

$$-r_{CO} = \frac{kP_{O_2}}{\left(1 + K_1 P_{CO}\right)^2} \tag{4.11}$$

Table 4.3. Elementary step reaction path for CO oxidation by O_2 over Pt-SnO_2/γ-Al_2O_3 in the absence of CO_2 and H_2O in the feed (Akın *et al.,* 2001)

Elementary Step	Step Number
$CO + * \underset{k_1^b}{\overset{k_1^f}{\Leftrightarrow}} CO*$	(1)
$O_2 + 2\blacksquare \underset{k_2^b}{\overset{k_2^f}{\Leftrightarrow}} 2O\blacksquare$	(2)
$CO* + O\blacksquare \overset{k_3^f}{\rightarrow} CO_2 + * + \blacksquare$	(3)

Oran and Uner (2004) proposed a mechanism for CO oxidation over Pt/CeO_2/γ-Al_2O_3 in the absence of CO_2 and H_2O in the feed. In their mechanism, CO adsorbs on the Pt sites and O_2 adsorbs molecularly on a single ceria site, followed by its dissociation. Then, the adsorbed oxygen passes to a Pt site, and CO_2 formation occurs by means of a Langmuir-Hinshelwood type surface reaction between adsorbed CO and oxygen. The mechanism is given in Table 4.4 in which "*" refers to the Pt sites, and "●" refers to the ceria sites. Assuming that CO coverage on the Pt sites is nearly 1, the rate-limiting step is the oxygen exchange at the ceria and Pt interface, i.e. step (3) in Table 4.4, and the surface coverage of oxygen over ceria is independent of the gas phase oxygen partial pressure, the rate expression takes its final form as below.

$$r_{CO_2} = \frac{k_2^f \theta_{O\bullet}}{1 + K_1 P_{CO}} \tag{4.12}$$

The last rate expression tested was taken from the kinetic study of Kahlich *et al.* (1997) without a mechanism proposal in a H_2-rich gas over Pt/Al_2O_3. They obtained the rate expression in Equation (4.13), by applying a power-law function to calculate the conversion of CO as a function of flow rate using estimated reaction orders.

$$-r_{CO} = k\left(P_{CO}\right)^{0.4}\left(\frac{2P_{O_2}}{P_{CO}}\right)^{0.82} \tag{4.13}$$

Table 4.4. Elementary step reaction path for CO oxidation by O_2 over $Pt\text{-}CeO_2/\gamma\text{-}Al_2O_3$ in the absence of CO_2 and H_2O in the feed (Oran and Uner, 2004)

Elementary Step	Step Number
$CO + * \underset{k_1^b}{\overset{k_1^f}{\Leftrightarrow}} CO*$	(1)
$O_2 + 2\bullet \overset{k_2^f}{\rightarrow} 2O\bullet$	(2)
$O\bullet + * \overset{k_3^f}{\rightarrow} O* + \bullet$	(3)
$CO* + O* \overset{k_4^f}{\rightarrow} CO_2 + 2*$	(4)

4.2. Experimental Results

CO conversion values for eight different feed compositions and two space times (W/F_{CO}) at a constant temperature, i.e. 110 °C, were used to obtain the corresponding CO consumption rates from intrinsic kinetic data in the initial rate region and the data were used for testing the rate expressions which were derived on the basis of mechanisms given in Table 4.2, or other rate equations from various studies in the literature. Also, additional experiments were conducted at two different temperatures, i.e. 120 °C and 130 °C, to evaluate the effect of temperature on the kinetic parameters.

4.2.1. The Effects of CO and O_2 Concentrations

The dependence of selective CO oxidation rate on CO and O_2 concentrations over Pt-Co-Ce/Al_2O_3 catalyst in the presence of 25 per cent CO_2 and 10 per cent H_2O, and in the absence of CO_2 and H_2O in the feed stream was studied. The results of the study are shown in Tables 4.5 and 4.6 respectively.

4.2.1.1. The Effects of CO and O_2 Concentrations with CO_2 and H_2O in the Feed. The inlet CO and O_2 concentrations, especially O_2/CO concentration ratio, required for efficient CO removal from hydrogen-rich stream by means of single-step selective CO oxidation, is the parameter of key importance.

As shown in Table 4.5, there is a significant effect of CO concentration at the reaction temperature studied. CO conversion decreases with increasing CO concentration in the feed. At 1.5 per cent CO in the feed, CO conversion reaches a minimum of 4.8 per cent for 10 mg catalyst and 7.5 per cent for 20 mg catalyst at 110 °C. This decrease may not be attributed to the lack of oxygen since the O_2 concentration is still above the stoichiometric ratio at 1.5 per cent CO where the CO conversion decreased most. The decrease with increasing CO concentration is most likely due to the well-known poisoning effect of CO on Pt sites (Luengnaruemitchai *et al.,* 2003).

The conversion of CO over Pt is well known to obey a single site Langmuir-Hinshelwood kinetic model, where O_2 and CO compete for the same sites. There is a decrease in reaction rate as the CO concentration is increased especially near the stoichiometric O_2/CO ratio of 0.5. Increasing concentrations of CO do not inhibit the reaction much. This result is consistent with a dual site non-competitive mechanism in which CO adsorbs onto the Pt sites and the O_2 dissociatively adsorbs onto the metal oxide site. Surface reaction occurs between CO and oxygen adatom on adjacent but different sites (Korotkikh and Farrauto, 2000).

The increase in O_2 concentration results in increasing CO conversion and reaction rate. This increase follows an almost straight trend for varying O_2 concentrations at a fixed CO concentration of 1 per cent.

Table 4.5. Results of kinetic experiments on CO oxidation kinetics for different CO and O_2 concentrations in the presence of 25% CO_2 and 10% H_2O measured at 60% H_2, and balance He, T = 110 °C

Exp. No.	CO (mol %)	O_2 (mol %)	O_2 : CO	$^{a}W_{CAT}$ / $^{b}F_{CO}$ (mg.s.μmol^{-1})	$^{c}X_{CO}$ (fractional)
1	1	0.5	0.5	18.868	0.032
2				37.736	0.094
3	1	0.75	0.75	18.868	0.063
4				37.736	0.102
5	1	1	1	18.868	0.079
6				37.736	0.121
7	1	1.25	1.25	18.868	0.081
8				37.736	0.142
9	1	1.5	1.5	18.868	0.088
10				37.736	0.149
11	0.75	1	1.33	25.157	0.087
12				50.314	0.211
13	1.25	1	0.8	15.094	0.058
14				30.189	0.096
15	1.5	1	0.67	12.579	0.048
16				25.157	0.075

[a]Catalyst weight, [b]CO flow, [c]CO conversion

4.2.1.2. The Effects of CO and O_2 Concentrations without CO_2 and H_2O in the Feed. CO conversion dropped from 23.2 per cent at 0.75 per cent CO to about 7.4 per cent at 1.5 per cent CO in the feed (Table 4.6). As a matter of fact, O_2 conversion also decreased from 23.3 per cent to 4.5 per cent with increasing CO concentrations. One possible explanation is that CO and oxygen are competing for active sites and that the higher concentration of CO is preventing the adsorption of oxygen on surface sites and hence its reaction with carbon monoxide or hydrogen (Özdemir *et al.,* 2004). This is evident from the fact that CO selectivity also increased with increasing CO concentration in the feed (Uysal, 2005).

The increase in O_2 concentration results in increasing CO conversion and reaction rate. It shows a similar trend as the feed with CO_2 and H_2O but at lower values. Park *et al*. (2004) stated that although it is very important to keep the O_2/CO ratio as low as possible to improve the fuel processing efficiency, at lower O_2/CO ratios, the presence of CO may block active sites by preferential binding, which decreases the sites for adsorption of O_2 and therefore lowers CO conversion.

Table 4.6. Results of kinetic experiments on CO oxidation kinetics for different CO and O_2 concentrations in the absence of CO_2 and H_2O measured at 60% H_2, and balance He, T = 110 °C

Exp. No.	CO (mol %)	O_2 (mol %)	O_2 : CO	$^{a}W_{CAT}$ / $^{b}F_{CO}$ (mg.s.μmol^{-1})	$^{c}X_{CO}$ (fractional)
1	1	0.5	0.5	18.868	0.073
2				37.736	0.127
3	1	0.75	0.75	18.868	0.071
4				37.736	0.147
5	1	1	1	18.868	0.062
6				37.736	0.167
7	1	1.25	1.25	18.868	0.078
8				37.736	0.175
9	1	1.5	1.5	18.868	0.092
10				37.736	0.185
11	0.75	1	1.33	25.157	0.097
12				50.314	0.232
13	1.25	1	0.8	15.094	0.064
14				30.189	0.119
15	1.5	1	0.67	12.579	0.052
16				25.157	0.074

The CO consumption rates for the feed containing CO_2 and H_2O were found to be smaller than the rates for the feed without CO_2 and H_2O. It seems that frequently reported enhancement effect of H_2O on the CO consumption rate (Manasilp and Gulari, 2002;

Rajasree *et al.,* 2004) is less than the inhibitory effect of CO_2 (Epling *et al.,* 2003; Avgouropoulos *et al.,* 2002). Kim and Lim (2002) reported that addition of H_2O to the dry feed mixture over Pt/Al_2O_3 does not affect the CO conversion while many authors stated that CO_2 addition to the feed results in decreased CO conversions (Nibbelke *et al.,* 1997; Uysal, 2005).

4.3. Determination of the Plausible Mechanisms

4.3.1. Rate Calculations

Rates of CO consumption have been evaluated using the differential method explained in Section 2.5.1. The experimental conditions were fixed to keep the CO conversions at low values, e.g. less than 20 per cent. It is reported that the differential reactor approximation could be used at conversions lower than 20 per cent to calculate reaction rates (Cant and Ossipoff, 1997; Han *et al.,* 2004). Even, necessity of conversions below 10 per cent is also reported (Nibbelke *et al.,* 1997; Kim and Lim, 2002).

The reaction rates were calculated from the slopes of the CO conversion versus space time (W/F_{CO}) graphs. Evaluation of the CO consumption rate for a constant feed composition involves experiments at constant flow with different catalyst loadings, and hence, different space times. The kinetic experiments have been repeated for eight different feed compositions at 110 °C, each at two different space times, to ensure that the data correspond to the linear change of CO conversion (X_{CO}) with space time (W/F_{CO}) in the initial rates region in which the reaction is kinetically controlled. The effect of the product CO_2 on the reaction rate was not considered since experiments were conducted in the region where low CO conversions were obtained and the data were extrapolated to zero space time.

Representative initial rate data extracted from 32 kinetic experiments, which are reported in Tables 4.5 and 4.6, by differentiation and extrapolation to zero space time as shown in Figures 4.1 and 4.2, are given in Tables 4.7 and 4.8.

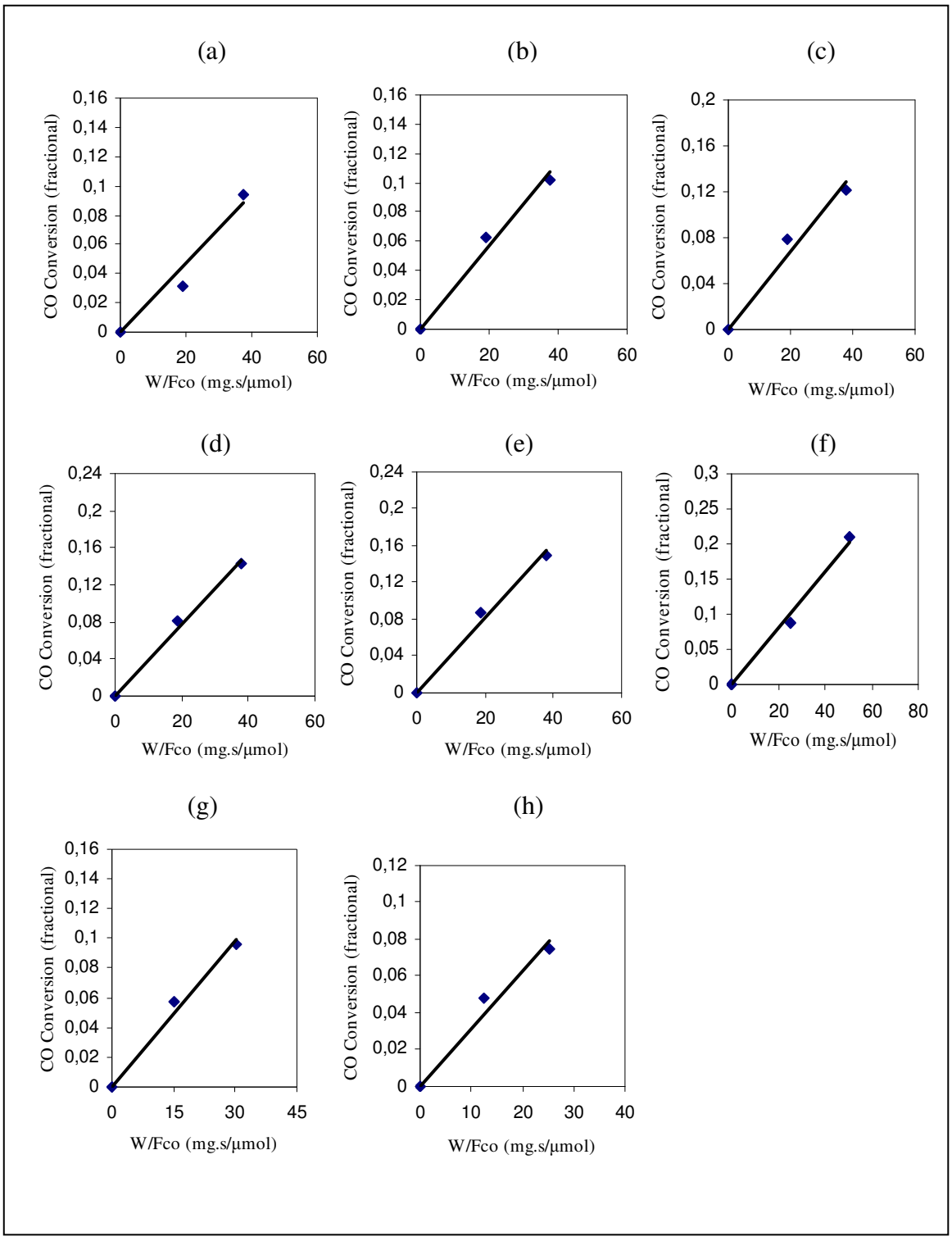

Figure 4.1. Fractional CO conversion vs. space time (W/F_{CO}) graphs: (a) 1% CO, 0.5 O_2; (b) 1% CO, 0.75 O_2; (c) 1% CO, 1% O_2; (d) 1% CO, 1.25% O_2; (e) 1% CO, 1.5% O_2; (f) 0.75% CO, 1% O_2; (g) 1.25% CO, 1% O_2; (h) 1.5% CO, 1% O_2 with 60% H_2, and the rest He in the presence of 25% CO_2 and 10% H_2O in the feed

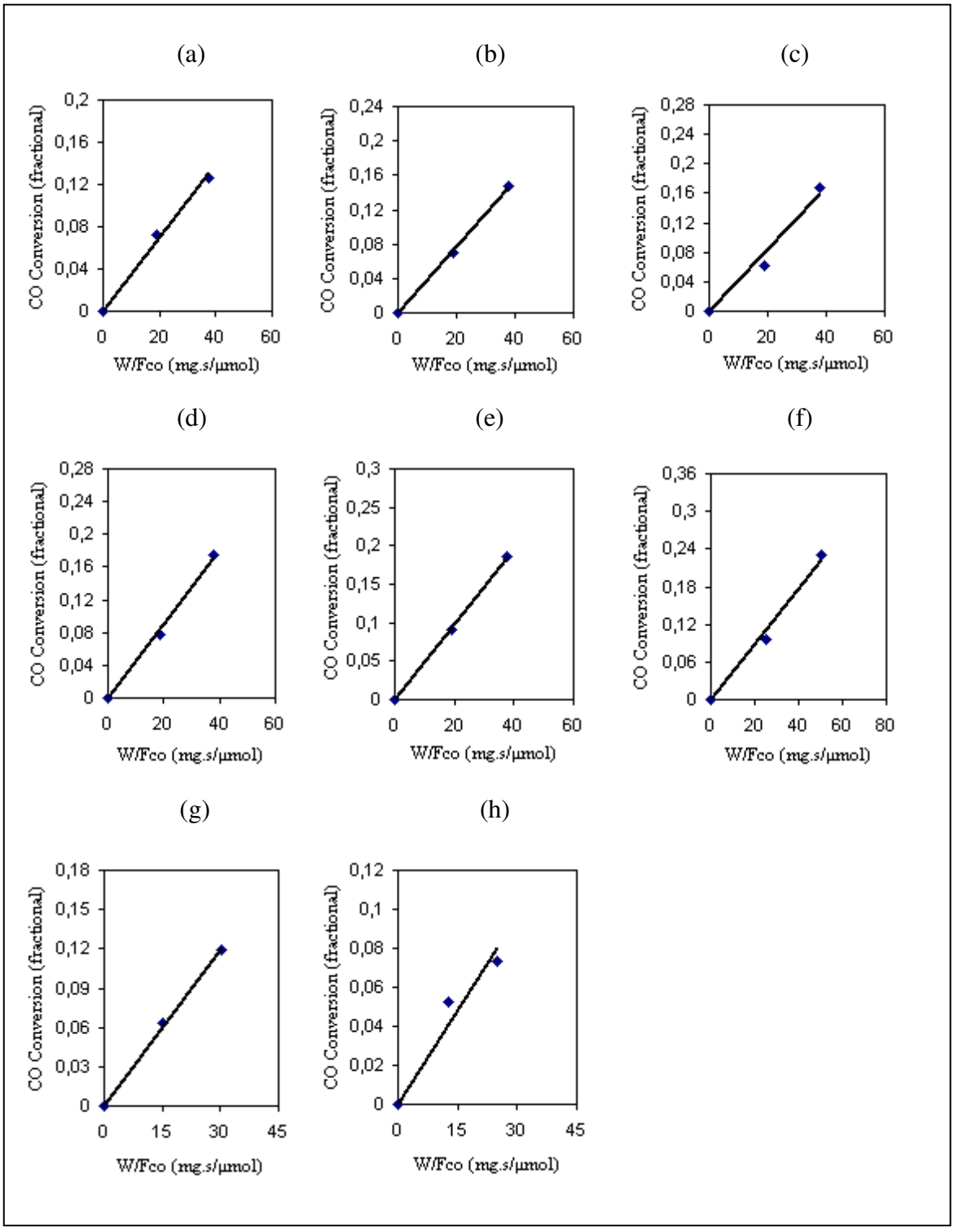

Figure 4.2. Fractional CO conversion vs. space time (W/F_{CO}) graphs: (a) 1% CO, 0.5 O_2; (b) 1% CO, 0.75 O_2; (c) 1% CO, 1% O_2; (d) 1% CO, 1.25% O_2; (e) 1% CO, 1.5% O_2; (f) 0.75% CO, 1% O_2; (g) 1.25% CO, 1% O_2; (h) 1.5% CO, 1% O_2 with 60% H_2, and the rest He in the absence of CO_2 and H_2O in the feed

Table 4.7. Initial rates calculated from CO conversion vs. space time (W/F_{CO}) data in the presence of 25% CO_2 and 10% H_2O, measured at 60% H_2, and balance He, T=110 °C

Experiment No.	CO (mol %)	O_2 (mol %)	Reaction rate (μmol $mg^{-1}s^{-1}$)
1-2	1	0.5	0.0023
3-4	1	0.75	0.0028
5-6	1	1	0.0034
7-8	1	1.25	0.0039
9-10	1	1.5	0.0041
11-12	0.75	1	0.0040
13-14	1.25	1	0.0033
15-16	1.5	1	0.0031

Table 4.8. Initial rates calculated from CO conversion vs. space time (W/F_{CO}) data in the absence of CO_2 and H_2O, measured at 60% H_2, and balance He, T=110 °C

Experiment No.	CO (mol %)	O_2 (mol %)	Reaction rate (μmol $mg^{-1}s^{-1}$)
1-2	1	0.5	0.0035
3-4	1	0.75	0.0039
5-6	1	1	0.0042
7-8	1	1.25	0.0045
9-10	1	1.5	0.0049
11-12	0.75	1	0.0045
13-14	1.25	1	0.0040
15-16	1.5	1	0.0032

4.3.2. Model Discrimination and Parameter Estimation

The concentrations given in mole per cent were converted into partial pressures, since the total pressure (ca. 1 atm = 101325 Pa) were also recorded at each experiment. The resulting rate data at each concentration set obtained at 110 °C were used to estimate the rate constants shown in the rate expressions of the proposed reaction paths using nonlinear regression analysis.

Nonlinear least squares method was preferred to linear least squares method because not all the models could be linearized and linear least squares method may yield false negative parameters when one or more independent variables appear in grouped dependent variable (Akın, 1996). The Levenberg-Marquardt regression scheme provided in the LSQNONLIN subroutine function in computer software MATLAB 7.0.4 (2005) which is a subspace trust region method and is based on the interior-reflective Newton method, was used for this purpose. This scheme estimates the specified parameters at the optimum point after some iterations. Each iteration involves the approximate solution of a large linear system using the method of preconditioned conjugate gradients. The optimum obtained may be either local or global depending on the initial guesses. Thus, initial guesses are important. Estimation of the kinetic parameters was performed by minimization of the following objective function:

$$S(b) = \sum_{i=1}^{n} \left[y_i - g(x_i, b) \right]^2 \rightarrow \text{minimum} \qquad (4.14)$$

where S is the objective function, b is the parameter vector; y_i is the ith experimental observation, which is the fractional CO conversion for the experiments with Pt-Co-Ce/γ-Al_2O_3, $g(x_i,b)$ is the corresponding value calculated by the model, x_i is the vector of set variables for experiment i, and n is the number of experiments. The objective function is based upon the assumption that the experimental errors are normally distributed with a zero mean.

The kinetic data presented in Tables 4.7 and 4.8 were used for testing the models listed in Sections 4.1.1 to 4.1.6. The criterion commonly used in model discrimination

requires that the parameters be positive. Statistical fitness of the calculated rate data with the experimental rate data are also frequently tested for model discrimination. The results obtained for the eleven models in question in the order as given in Sections 4.1.1 to 4.1.6 are given in Tables 4.9 and 4.10.

Table 4.9. The obtained results for the model parameters for the feed containing 25% CO_2 and 10% H_2O

Model Eqn. / Parameters	4.3	4.4	4.5	4.6	4.7	4.8	4.9	4.10	4.11	4.12	4.13
K1	(+)	(+)	(+)	(+)	(+)	(-)	(-)	(-)	(+)	(+)	(+)
K2	(+)	(-)	(+)	(+)	(-)	(-)	(-)	(+)	(+)	(+)	-
K3	(+)	(+)	-	-	(-)	-	-	-	-	-	-
K4	(+)	(-)	-	-	(+)	-	-	-	-	-	-
K5	(+)	-	-	-	-	-	-	-	-	-	-

Table 4.10. The obtained results for the model parameters for the feed containing no CO_2 and H_2O

Model Eqn. / Parameters	4.3	4.4	4.5	4.6	4.7	4.8	4.9	4.10	4.11	4.12	4.13
K1	(+)	(+)	(+)	(+)	(+)	(-)	(-)	(-)	(+)	(+)	(+)
K2	(+)	(-)	(+)	(+)	(-)	(-)	(-)	(+)	(+)	(+)	-
K3	(+)	(+)	-	-	(-)	-	-	-	-	-	-
K4	(+)	(-)	-	-	(+)	-	-	-	-	-	-
K5	(+)	-	-	-	-	-	-	-	-	-	-

Equivalents of the parameters that were estimated by the MATLAB code in terms of the parameters defined in the model equations are listed in Table 4.11.

Table 4.11. The equivalents of the parameters defined in the model equations

Parameters / Model Eqn.	K1	K2	K3	K4	K5
4.3	K_1	k_4^f	$k_9^f [S]_0$	k_3^f	k_9^f
4.4	k_7^f	k_8^f	$k_8^f [S]_0$	$k_3^f [S]_0$	-
4.5	$k_5^f [V]_0$	$k_{10}^f [S]_0 [V]_0$	-	-	-
4.6	$k_5^f [V]_0$	K_2	-	-	-
4.7	K_1	$k_3^f [S]_0$	$k_{10}^f [V]_0$	$k_{10}^f [S]_0 [V]_0$	-
4.8	k_5^f	k_2^f	-	-	-
4.9	k_5^f	K_2	-	-	-
4.10	k_3^f	k_5^f	-	-	-
4.11	k	K_1	-	-	-
4.12	$k_2^f \theta_{O\bullet}$	K_1	-	-	-
4.13	k	-	-	-	-

According to the results in Tables 4.9 and 4.10, the models including negative parameters were eliminated. In order to compare the remaining models, which comprise of only positive parameters, fitness of the calculated values of the rates with the experimental rates were tested. The results are displayed in Figures 4.3 and 4.4 for the model equations in the presence of 25 per cent CO_2 and 10 per cent H_2O, and in the absence of CO_2 and H_2O in the feed, respectively.

By taking the regression coefficients from the Figures 4.3 and 4.4 into consideration, only the model given by the Equation (4.12) seems to show a discord with the experimental results. All the other models with positive parameters, i.e. models given by the Equations (4.3), (4.5), (4.6), (4.11) and (4.13), do not differ significantly as far as regression coefficients are concerned.

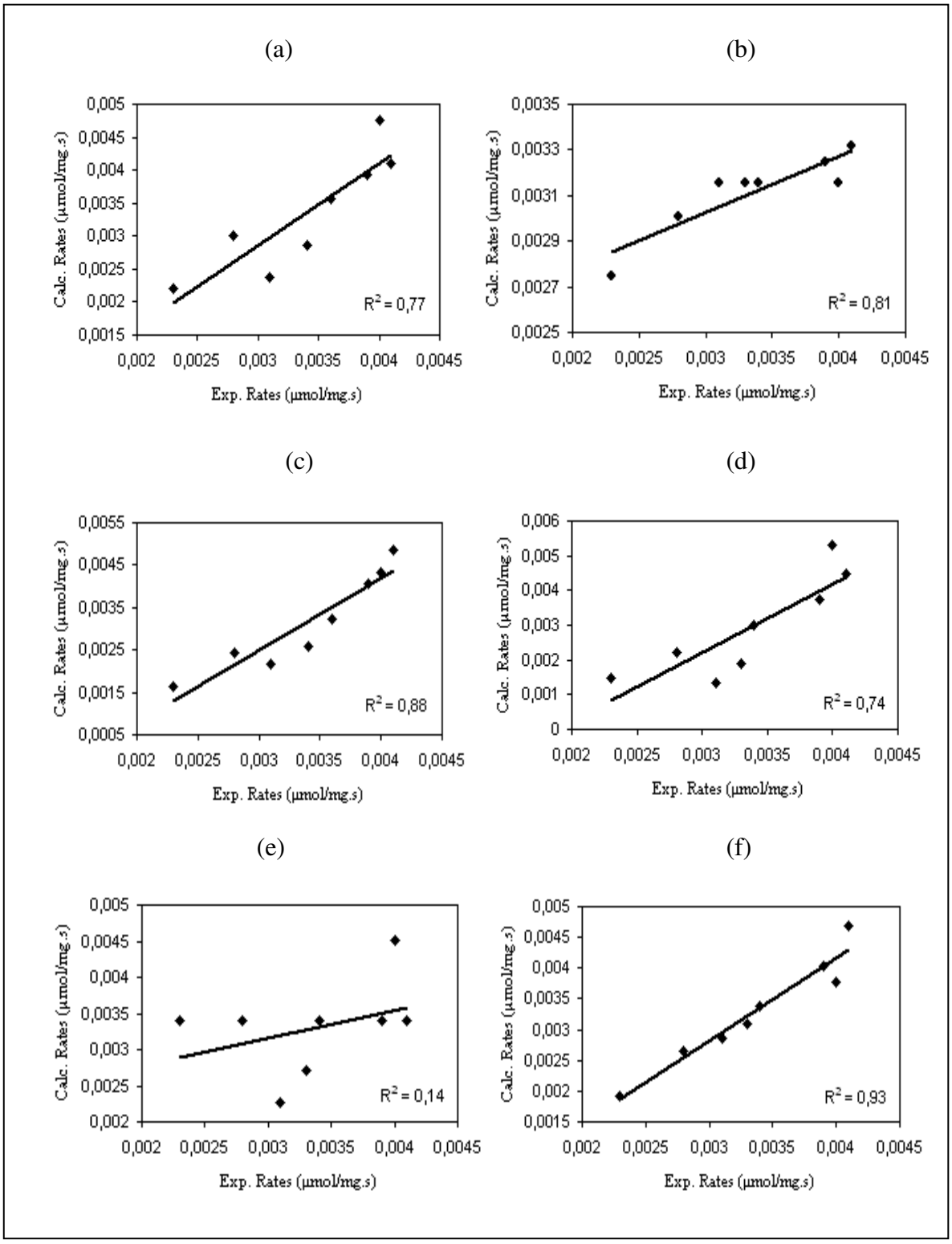

Figure 4.3. Calculated rates vs. experimental rates for the model equations in the presence of 25% CO_2 and 10% H_2O in the feed: (a) Eqn. (4.3); (b) Eqn. (4.5); (c) Eqn. (4.6); (d) Eqn. (4.11); (e) Eqn. (4.12); (f) Eqn. (4.13)

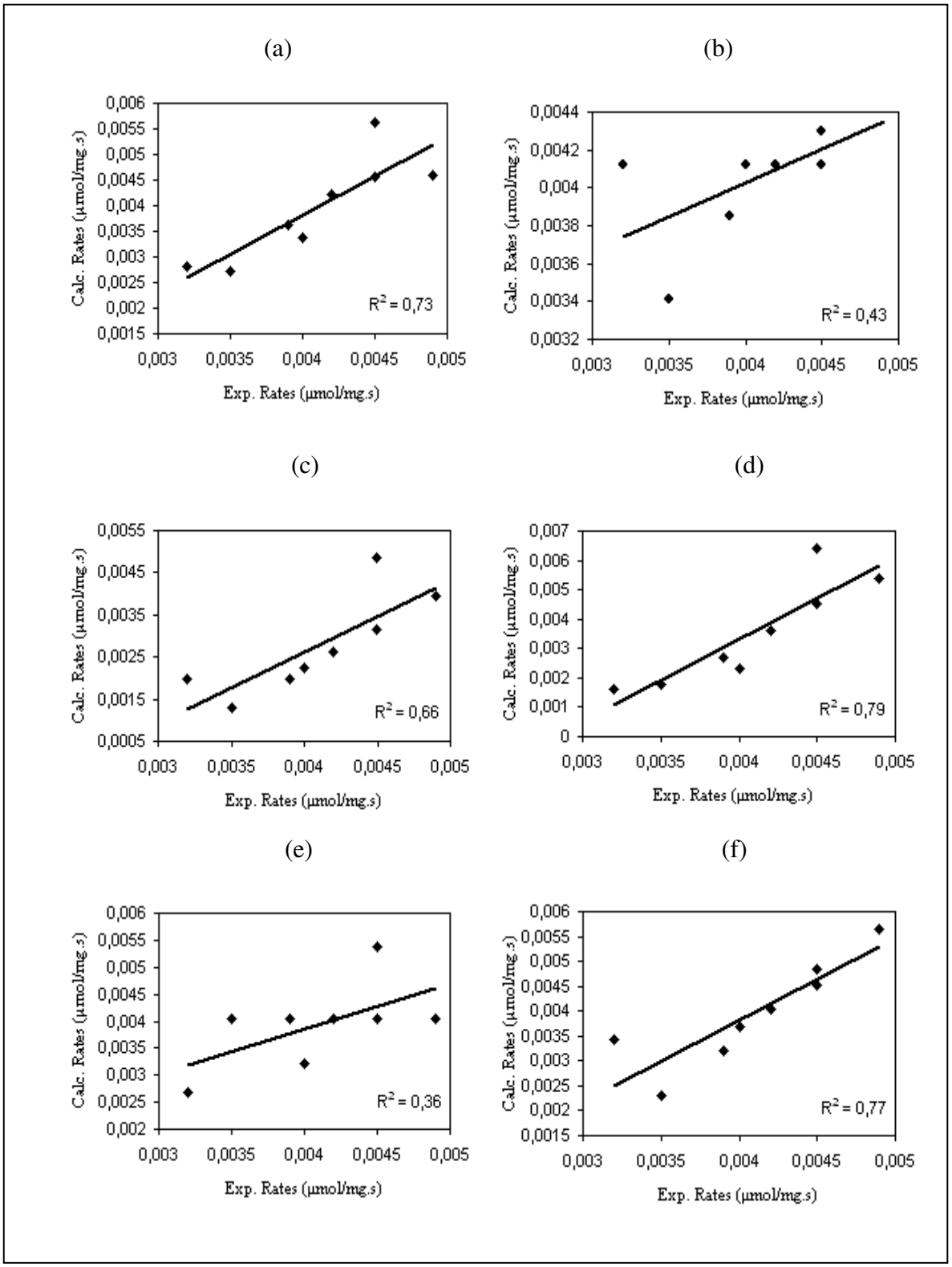

Figure 4.4. Calculated rates vs. experimental rates for the model equations in the absence of CO_2 and H_2O in the feed: (a) Eqn. (4.3); (b) Eqn. (4.5); (c) Eqn. (4.6); (d) Eqn. (4.11); (e) Eqn. (4.12); (f) Eqn. (4.13)

Model discrimination leading to the estimation of positive parameters which also give a good statistical fit of the data is a necessary but not sufficient requirement for deciding on a particular reaction mechanism. Because of that, apart from the nonlinear regression analysis, the effect of temperature on the reaction rates was also investigated. An Arrhenius plot (Figure 4.5) was used for this purpose to check the behavior of the rate towards varying temperatures. Additional experiments were conducted with the feed containing 1 per cent CO and 0.5 per cent O_2, i.e. stoichiometric feed, at 120 °C and 130 °C, and also using the existing rate data at 110 °C, to obtain necessary data for the plot and the results of the experiments are given in Table 4.12.

Table 4.12. Results of additional experiments on CO oxidation kinetics for the feed containing 1% CO and 0.5% O_2 at different reaction temperatures in the presence of 25% CO_2 and 10% H_2O measured at 60% H_2, and balance He

Temperature (°C)	$^{a}W_{CAT}$ / $^{b}F_{CO}$ (mg.s.µmol^{-1})	$^{c}X_{CO}$ (fractional)	Reaction rate (µmol.mg^{-1}s^{-1})
120	18.868	0.066	0.0039
120	37.736	0.149	
130	18.868	0.093	0.0047
130	37.736	0.176	

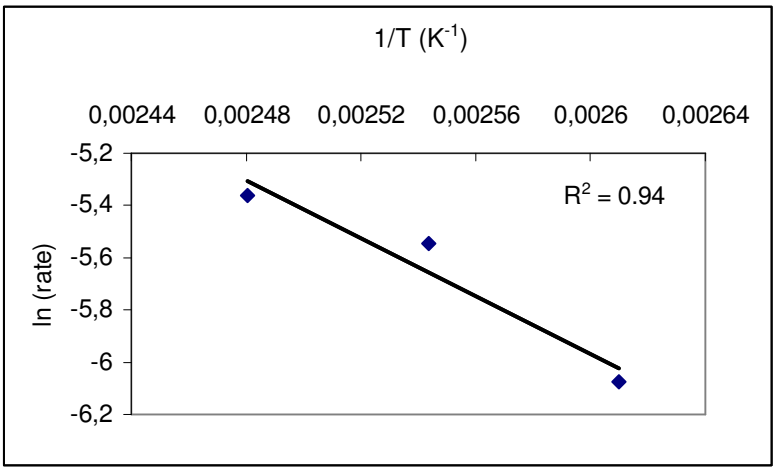

Figure 4.5. Arrhenius plot for the feed containing 1% CO and 0.5% O_2 in the presence of 25% CO_2 and 10% H_2O measured at 60% H_2, and balance He

As can be seen from Figure 4.5, the form of the Arrhenius plot shows a linear relation. Assuming that the dependence of equilibrium constants to temperature is lower than the dependence of rate constants, it might be accepted that the models given by the Equations (4.5), (4.6), (4.11) and (4.13) show a better correlation with the form of the Arrhenius plot, when the form of the five model equations in question is taken into consideration. Hence, the selection of the monofunctional mechanism as a plausible mechanism might be unreasonable. This is also supported with the fact that increasing CO concentrations do not inhibit the reaction much, indicating the validity of a dual site mechanism (Korotkikh and Farrauto, 2000).

From a statistical point of view, the models given by the Equations (4.3), (4.5), (4.6), (4.11) and (4.13) are equally suited for describing the experiments, as the regression coefficients do not differ significantly. In the literature, there are several other studies are present where alternative model equations giving similar results that could not be distinguished statistically (Nibbelke *et al.,* 1997; Nibbelke *et al.,* 1998). The estimated kinetic parameters for all of the plausible models are listed in Tables 4.13 and 4.14.

Table 4.13. The calculated parameters for the model equations in the presence of 25% CO_2 and 10% H_2O in the feed

Model Eqn. / Parameters	4.3	4.5	4.6	4.11	4.13
K1	0.8923 $\left(1/Pa\right)$	3.3×10^{-6} $\left(\frac{\mu mol}{Pa.mg.s}\right)$	0.0357 $\left(\frac{\mu mol}{Pa.mg.s}\right)$	0.3707 $\left(\frac{\mu mol}{Pa.mg.s}\right)$	1.04×10^{-4} $\left(\frac{\mu mol}{Pa^{0.4}.mg.s}\right)$
K2	1.6338 $\left(\frac{mg}{\mu mol.s}\right)$	0.0069 $\left(\frac{\mu mol}{mg.s}\right)$	22.0388 $\left(1/Pa\right)$	0.3492 $\left(1/Pa\right)$	-
K3	1.2991 $\left(1/s\right)$	-	-	-	-
K4	0.0011 $\left(1/Pa.s\right)$	-	-	-	-
K5	0.6076 $\left(\frac{mg}{\mu mol.s}\right)$	-	-	-	-

Table 4.14. The calculated parameters for the model equations in the absence of CO_2 and H_2O in the feed

Parameters \ Model Eqn.	4.3	4.5	4.6	4.11	4.13
K1	0.8829 $\left(1/Pa\right)$	9.8×10^{-6} $\left(\frac{\mu mol}{Pa.mg.s}\right)$	0.0127 $\left(\frac{\mu mol}{Pa.mg.s}\right)$	0.6971 $\left(\frac{\mu mol}{Pa.mg.s}\right)$	1.25×10^{-4} $\left(\frac{\mu mol}{Pa^{0.4}.mg.s}\right)$
K2	1.6551 $\left(\frac{mg}{\mu mol.s}\right)$	0.0052 $\left(\frac{\mu mol}{mg.s}\right)$	2.5210 $\left(1/Pa\right)$	0.4360 $\left(1/Pa\right)$	-
K3	1.3179 $\left(1/s\right)$	-	-	-	-
K4	0.0013 $\left(1/Pa.s\right)$	-	-	-	-
K5	0.5883 $\left(\frac{mg}{\mu mol.s}\right)$	-	-	-	-

It should be noted that only steady state experiments were carried out in this work. These types of experiments do not determine the individual coverages of species on the catalyst surface that underlie any mechanism. Moreover, the accessible kinetic parameters consist of combinations of the rate coefficients of individual elementary steps (Hoebink *et al.,* 1997). For these reasons, proposed mechanisms are simplified cases for the actual reaction pathway, still they are good representations for understanding the synergy between the constituents of the catalyst.

As a result, five models were chosen as the plausible kinetic models among the eleven models, as no distinction could be made between them statistically. Three of those mechanisms are bifunctional, in which adsorption of CO and O_2 takes place on different sites and formation of CO_2 proceeds via Langmuir-Hinshelwood type surface reactions, one of them is a model without a proposed mechanism, and one of them is a monofunctional mechanism proceeding on the platinum sites only.

5. CONCLUSIONS AND RECOMMENDATIONS

5.1. Conclusions

Kinetics of low temperature CO oxidation was studied in hydrogen-rich streams with a realistic gas composition using cobalt and ceria promoted Pt/Al_2O_3 catalyst prepared by incipient-to-wetness impregnation. Intrinsic kinetic data were obtained in the initial rate region in a microflow reactor operating in differential mode using eight different sets of CO and O_2 concentrations each at two residence times, i.e. two catalyst loadings, at 110 °C both in the presence of 25 per cent CO_2 and 10 per cent H_2O, and in the absence of CO_2 and H_2O. The effect of temperature on the reaction rates was also investigated in the range of 110-130 °C. The experimental rate data were used to estimate the kinetic parameters of the model equations for the mechanisms proposed in this study, and for six alternative mechanisms from other studies in the literature. Model discrimination between all the model equations tested was carried out by comparing the calculated data with the experimental data. The major conclusions that can be drawn from this study are given as follows:

- By taking the fitness of the calculated rates of the models which comprise of only positive parameters, with the experimental rates into consideration, five models were chosen as the plausible kinetic models among the eleven models, as no distinction could be made between them statistically. Three of those mechanisms are bifunctional, in which adsorption of CO and O_2 takes place on different sites and formation of CO_2 proceeds via Langmuir-Hinshelwood type surface reactions, one of them is a model without a mechanism proposal, and one of them is a monofunctional mechanism proceeding on the platinum sites only.
- For the five plausible models, no significant differences were observed between the experiments in the presence of CO_2 and H_2O, and in the absence of CO_2 and H_2O when the fitness of the calculated rate data with the experimental rate data is considered.
- The Arrhenius plot that was used to see the effect of temperature on the reaction rates showed a linear relation (R^2 = 0.94) in the temperature range of 110-130 °C.

Assuming that the dependence of equilibrium constants to temperature is lower than the dependence of rate constants, it could be seen that the monofunctional model given by the Equation (4.3) shows less correlation with the form of the Arrhenius plot, when the form of the five model equations in question is taken into consideration. Hence, the selection of the monofunctional mechanism as a plausible mechanism might be unreasonable.

5.2. Recommendations

Under the light of the results of the present work, the following studies are recommended for further studies:

- Kinetic experiments may be conducted at higher space times using pure and mixed feeds in order to clarify the reaction mechanism and to obtain rate expressions that are more generally applicable.
- Kinetic analysis of the experimental data of the present study may be repeated using the integral method by adding the necessary experimental data in order to make a discrimination between the plausible models found in this work.
- Kinetic studies may be repeated and improved by performing several experiments at different temperatures to calculate the activation energy of the CO oxidation reaction, and hence, to obtain the effect of temperature on the mechanism over Co-Ce promoted Pt/Al_2O_3 catalyst.
- Quantum chemical methods may be used to clarify the molecular level properties of the active sites or the metal-support interfaces, which directly contribute to the elucidation of the CO oxidation mechanism over the Co-Ce promoted Pt/Al_2O_3 catalyst.

REFERENCES

Akın, A. N., G. Kılaz, A. İ. İşli and Z. İ. Önsan, 2001, "Development and Characterization of Pt-SnO_2/γ-Al_2O_3 Catalysts", *Chemical Engineering Science*, Vol. 56, pp. 881-888.

Akın, A. N., 1996, *Development of Coprecipitated Cobalt-Alumina Catalysts for the Production of C_1-C_4 Hydrocarbons by Carbon Monoxide Hydrogenation*, Ph. D. Thesis, Boğaziçi University.

Avgouropoulos, G., T. Ioannides, C. H. Papadopoulou, J. Batista, S. Hocevar and H. K. Matralis, 2002, "A Comparative Study of Pt/γ-Al_2O_3, Au/α-Fe_2O_3 and CuO-CeO_2 Catalysts for the Selective Oxidation of Carbon Monoxide in Excess Hydrogen", *Catalysis Today,* Vol. 75, pp. 157-167.

Bunluesin, T., R. J. Gorte and G. W. Graham, 1998, "Studies of the Water-Gas-Shift Reaction on Ceria-Supported Pt, Pd, and Rh: Implications for Oxygen-Storage Properties", *Applied Catalysis B: Environmental*, Vol. 15, pp. 107-l 14.

Cant, N. W. and N. J. Ossipoff, 1997, "Cobalt Promotion of Au/TiO_2 Catalysts for the Reaction of Carbon Monoxide with Oxygen and Nitrogen Oxides", *Catalysis Today*, Vol. 36, pp. 125-133.

Carlsson, P. A., L. Österlund, P. Thormählen, A. Palmqvist, E. Fridell, J. Jansson and M. Skoglundh, 2004, "A Transient in situ FTIR and XANES Study of CO Oxidation over Pt/Al_2O_3 Catalysts", *Journal of Catalysis*, Vol. 226, pp. 422-434.

Carlsson, P. A., V. P. Zhdanova and B. Kasemo, 2005, "Bistable Mean-Field Kinetics of CO Oxidation on Pt with Oxide Formation", *Applied Surface Science*, Vol. 239, pp. 424-431.

Choi, Y. and H. G. Stenger, 2004, "Kinetics, Simulation and Insights for CO Selective Oxidation in Fuel Cell Applications", *Journal of Power Sources*, Vol. 129, pp. 246-254.

Choudhary, T. V. and D. W. Goodman, 2002, "CO-Free Fuel Processing for Fuel Cell Applications", *Catalysis Today*, Vol. 77, pp. 65–78.

Damyanova, S. and J. M. C. Bueno, 2003, "Effect of CeO_2 Loading on the Surface and Catalytic Behaviors of CeO_2-Al_2O_3-Supported Pt Catalysts", *Applied Catalysis A: Genera,* Vol. 253, pp.135-150.

Demmin, R. A. and R. J. Gorte, 1987, "A Study of Methanation Kinetics on a Clean and a Titania-Covered Platinum Foil", *Journal of Catalysis*, Vol. 105, pp. 373-385.

Dudfield, C. D., R. Chen and P. L. Adcock, 2001, "A Carbon Monoxide PROX Reactor for PEM Fuel Cell Automotive Application", *International Journal of Hydrogen Energy*, Vol. 26, pp. 763-775.

Epling, W. S., P. K. Cheekatamarla and A. M. Lane, 2003, "Reaction and Surface Characterization Studies of Titania-Supported Co, Pt and Co/Pt Catalysts for the Selective Oxidation of CO in H_2-Containing Streams", *Chemical Engineering Journal*, Vol. 93, pp. 61-68.

El-Shobaky, G. A. and N. M. Deraz, 2001, "Surface and Catalytic Properties of Cobaltic Oxide Supported on an Active Magnesia", *Thermochimica Acta*, Vol. 375, pp. 137-145.

El-Shobaky, G. A., A. S. Ahmed, G. A. Fagal and M. Mokhtar, 1998, "Solid–Solid Interaction in CuO-ZnO/Al_2O_3 System under Varying Conditions", *Thermochimica Acta*, Vol. 319, pp. 67-74.

Fogler, H. S., 1992, *Elements of Chemical Reaction Engineering*, Prentice-Hall, Englewood Cliffs, New Jersey.

Froment G. F. and K. B. Bischoff, 1990, *Chemical Reactor Analysis and Design*, Wiley, New York.

Gray, P. G. and J. C. Frost, 1998, "Impact of Catalysis on Clean Energy in Road Transportation", *Energy & Fuels*, Vol. 12, pp. 1121-1129.

Han, Y. F., M. Kinne and R.J. Behm, 2004, "Selective Oxidation of CO on Ru/γ-Al_2O_3 in Methanol Reformate at Low Temperatures", *Applied Catalysis B: Environmental*, Vol. 52, pp. 123-134.

Hasegawa, Y., A. Ueda, K. Kusakabe and S. Morooka, 2002, "Oxidation of CO in Hydrogen-Rich Gas Using a Novel Membrane Combined with a Microporous SiO_2 Layer and a Metal-Loaded γ-Al_2O_3 Layer", *Applied Catalysis A: General*, Vol. 225, pp. 109-115.

Hilaire, S., X. Wanga, T. Luoa, R. J. Gorte and J. Wagner, 2001, "A Comparative Study of Water-Gas-Shift Reaction over Ceria Supported Metallic Catalysts", *Applied Catalysis A: General*, Vol. 215, pp. 271-278.

Holmgren, A., F. Azarnoush and E. Fridell, 1999, "Influence of Pre-Treatment on the Low-Temperature Activity of Pt/Ceria", *Applied Catalysis B: Environmental*, Vol. 22, pp. 49-61.

Hightower, J. W., B. Delmon, P. A. Jacobs and G. Poncelet, 1976, *Preparation of Catalysts I*, Elsevier, Amsterdam.

Hoebink, J. H. B. J., J. M. A. Harmsen, M. Balenovic, A. C. P. M. Backx and J. C. Schouten, 2001, "Automotive Exhaust Gas Conversion: From Elementary Step Kinetics to Prediction of Emission Dynamics", *Topics in Catalysis*, Vol. 16/17, No. 1-4, pp. 319-327.

Hoebink, J. H. B. J., J. P. Huinink, and G. B. Marin, 1997, "A Quantitative Analysis of Transient Kinetic Experiments: The Oxidation of CO by O_2 over Pt", *Applied Catalysis A: General*, Vol. 160, pp. 139-151.

Igarashi, H., H. Uchida, M. Suzuki, Y. Sasaki and M. Watanabe, 1997, "Removal of Carbon Monoxide from Hydrogen-Rich Fuels by Selective Oxidation over Platinum Catalyst Supported on Zeolite", *Applied Catalysis A: General*, Vol. 159, pp. 159-169.

İnce, T., 2004, *Low Temperature Oxidation of Carbon Monoxide over Pt-CeO_2-Co_3O_4/Al_2O_3 Catalyst in H_2-Rich Streams*, M. S. Thesis, Boğaziçi University.

Jansson, J., 2000, "Low-Temperature CO Oxidation over Co_3O_4/Al_2O_3", *Journal of Catalysis,* Vol. 194, pp. 55-60.

Jansson J., M. Skoglundh, E. Fridell and P. Thormählen, 2001, "A Mechanistic Study of Low Temperature CO Oxidation over Cobalt Oxide", *Topics in Catalysis*, Vol. 16/17, No. 1-4, pp. 385-389.

Johansson, S., L. Österlund, and B. Kasemo, 2001, "Oxidation Bistability Diagrams for Pt/CeO_x and Pt/SiO_2 Model Catalysts Prepared by Electron-Beam Lithography", *Journal of Catalysis*, Vol. 201, pp. 275-285.

Kahlich, M., J. H. A. Gasteiger and R. J. Behm, 1997, "Kinetics of the Selective CO Oxidation in H_2-Rich Gas on Pt/Al_2O_3", *Journal of Catalysis*, Vol. 171, pp. 93-105.

Kim, D. H. and M. S. Lim, 2002, "Kinetics of Selective CO Oxidation in Hydrogen-Rich Mixtures on Pt/Alumina Catalysts", *Applied Catalysis A: General*, Vol. 224, pp. 27-38.

Korotkikh, O. and R. Farrauto, 2000, "Selective Catalytic Oxidation of CO in H_2: Fuel Cell Applications", *Catalysis Today*, Vol. 62, pp. 249-254.

Kwak, C., T. J. Park and D. J. Suh, 2005, "Preferential Oxidation of Carbon Monoxide in Hydrogen-Rich Gas over Platinum-Cobalt-Alumina Aerogel Catalysts", *Chemical Engineering Science*, Vol. 60, pp. 1211-1217.

Lin, H. K., H. C. Chiu, H. C. Tsaia, S. H. Chien and C. B. Wang, 2003, "Synthesis, Characterization and Catalytic Oxidation of Carbon Monoxide over Cobalt Oxide", *Catalysis Letters*, Vol. 88, Nos. 3-4.

Liu, X., O. Korotkikh and R. Farrauto, 2002, "Selective Catalytic Oxidation of CO in H_2: Structural Study of Fe Oxide-Promoted Pt/Alumina Catalyst", *Applied Catalysis A: General*, Vol. 226, pp. 293-303.

Luengnaruemitchai, A., S. Osuwan and E. Gulari, 2003, "Comparative Studies of Low-temperature Water-Gas Shift Reaction over Pt/CeO_2, Au/CeO_2, and Au/Fe_2O_3 catalysts", *Catalysis Communications*, Vol. 4, pp. 215-221.

Manasilp, A. and E. Gulari, 2002, "Selective CO Oxidation over Pt/Alumina Catalysts for Fuel Cell Applications", *Applied Catalysis B: Environmental*, Vol. 37, pp. 17-25.

Manuel, I., J. Chaubet, C. Thomas, H. Colas, N. Matthess and G. D. Mariadassou, 2004, "Simulation of the Transient CO Oxidation over Rh^0/SiO_2 and $Rh^{x+}/Ce_{0.68}Zr_{0.32}O_2$ Catalysts", *Journal of Catalysis,* Vol. 224, pp. 269-277.

Mariño, F., C. Descorme and D. Duprez, 2004, "Noble Metal Catalysts for the Preferential Oxidation of Carbon Monoxide in the Presence of Hydrogen (PROX)", *Applied Catalysis B: Environmental*, Vol. 54, pp. 59-66.

Masel, R. I., 2001, *Chemical Kinetics and Catalysis*, Wiley-Interscience, New York.

MATLAB, Version 7.0.4, The MathWorks Inc., 2005.

Meng, M., P. Lin and Y. Fu, 1997, "The Catalytic Removal of CO and NO over Co-Pt(Pd, Rh)/γ-Al_2O_3 Catalysts and Their Structural Characterizations", *Catalysis Letters*, Vol. 48, pp. 213-222.

Mergler, Y. J., J. Hoebink, and B. E. Nieuwenhuys, 1997, "CO Oxidation over a Pt/CoO_x /SiO_2 Catalyst: A Study Using Temporal Analysis of Products", *Journal of Catalysis,* Vol. 167, pp. 305-313.

Nibbelke, R. H., M. A. J. Campman, J. H. B. J. Hoebink and G. B. Marin, 1997, "Kinetic Study of the CO Oxidation over Pt/γ-Al_2O_3 and Pt/Rh/CeO_2/γ-Al_2O_3 in the Presence of H_2O and CO_2", *Journal of Catalysis*, Vol. 171, pp. 358-373.

Nibbelke, R. H., A. J. L. Nievergeld, J. H. B. J. Hoebink and G. B. Marin, 1998, "Development of a Transient Kinetic Model for the CO Oxidation by O_2 over a Pt/Rh/CeO_2/γ-Al_2O_3 Three-Way Catalyst", *Applied Catalysis B: Environmental*, Vol. 19, pp. 245-259.

Oh, S. H. and R. M. Sinkevitch, 1993, "Carbon Monoxide Removal from Hydrogen-Rich Fuel Cell by Selective Catalytic Oxidation", *Journal of Catalysis*, Vol. 142, pp. 254-262.

Oleksenko, L. P., 2004, "Characteristics of Active Site Formation in Co-Containing Catalysts for CO Oxidation on Chemically Different Supports", *Theoretical and Experimental Chemistry*, Vol. 40, No. 5.

Oran, U. and D. Uner, 2004, "Mechanisms of CO Oxidation Reaction and Effect of Chlorine Ions on the CO Oxidation Reaction over Pt/CeO_2 and Pt/CeO_2/γ-Al_2O_3 catalysts", *Applied Catalysis B: Environmental,* Vol. 54, pp. 183-191.

Özdemir, C., A. N. Akın, and R. Yıldırım, 2004, "Low Temperature CO Oxidation in Hydrogen Rich Streams on Pt-SnO_2/Al_2O_3 Catalyst Using Taguchi Method", *Applied Catalysis A: General*, Vol. 258, pp. 145-152.

Özdemir, C., 2003, *Low Temperature CO Oxidation in Hydrogen-Rich Streams over Pt-SnO_2/Al_2O_3 Catalysts Prepared by Sol-Gel Method*, M. S. Thesis, Boğaziçi University.

Özkara, Ş., 2002, *Selective Low Temperature Carbon Monoxide Oxidation in H_2-Rich Gas Streams over Zeolite and Activated Carbon Supported Catalysts,* M. S. Thesis, Boğaziçi University.

Özkara, Ş. and A. E. Aksoylu, 2003, "Selective Low Temperature Carbon Monoxide Oxidation in H_2-Rich Gas Streams over Activated Carbon Supported Catalysts", *Applied Catalysis A: General*, Vol. 251, pp. 75-83.

Panzera, G., V. Modafferi, S. Candamanoa, A. Donato, F. Frusteri and P. L. Antonucci, 2004, "CO Selective Oxidation on Ceria-Supported Au Catalysts for Fuel Cell Application" *Journal of Power Sources*, Vol. 135, pp. 177-183.

Park, J. W., J. H. Jeong, W. L. Yoon, C. S. Kim, D. K. Lee, Y. K. Park and Y. W. Rhee, 2005, "Selective Oxidation of CO in Hydrogen-Rich Stream over Cu-Ce Catalyst Promoted with Transition Metals", *International Journal of Hydrogen Energy*, Vol. 30, pp. 209-220.

Park, J. W., J. H. Jeong, W. L. Yoon and Y. W. Rhee , 2004, "Selective Oxidation Of Carbon Monoxide in Hydrogen-Rich Stream over Cu-Ce/γ-Al_2O_3 Catalysts Promoted With Cobalt in a Fuel Processor for Proton Exchange Membrane Fuel Cells", *Journal of Power Sources*, Vol. 132, pp. 18-28.

Rajasree, R., J. H. B. J. Hoebink and J. C. Schouten, 2004, "Transient Kinetics of Carbon Monoxide Oxidation by Oxygen over Supported Palladium/Ceria/Zirconia Three-Way Catalysts in the Absence and Presence of Water and Carbon Dioxide", *Journal of Catalysis*, Vol. 223, pp. 36-43.

Roh, H. S., H. S. Potdar, K. W. Jun, S. Y. Han and J. W. Kim, 2004, "Low Temperature Selective CO Oxidation in Excess of H_2 over Pt/Ce-ZrO_2 Catalysts", *Catalysis Letters*, Vol. 93, No. 3-4.

Satterfield, C. N., 1991, *Heterogeneous Catalysis in Industrial Practice*, McGraw-Hill, USA.

Schmal, M., M. M. V. M. Souza, N. S. Resende, A. L. Guimarâes, C. A. Perez, J. G. Eon, D. A. G. Aranda and L. C. Dieguez, 2005, "Interpretation of Kinetic Data with Selected Characterizations of Active Sites", *Catalysis Today*, Article in Press.

Schubert, M. M., H. A. Gasteiger and R. J. Behm, 1997, "Surface Formates as Side Products in the Selective CO Oxidation on Pt/γ-Al_2O_3", *Journal of Catalysis*, Vol. 172, pp. 256-258.

Schubert, M. M., V. Plzak , J. Garche and R. J. Behm, 2001, "Activity, Selectivity, and Long-Term Stability of Different Metal Oxide Supported Gold Catalysts for the Preferential CO Oxidation in H_2-Rich Gas", *Catalysis Letters*, Vol. 76, pp. 143-150.

Sedmak, G., S. Hocevar and J. Levec, 2004, "Transient Kinetic Model of CO Oxidation over a Nanostructured $Cu_{0.1}Ce_{0.9}O_2$-Catalyst", *Journal of Catalysis*, Vol. 222, pp. 87-99.

Serre, C., F. Garin, G. Belot and G. Maire, 1993, "Reactivity of Pt/Al_2O_3 and Pt-CeO_2/ Al_2O_3 Catalysts for the Oxidation of Carbon Monoxide by Oxygen II. Influence of the Pretreatment Step on the Oxidation Mechanism", *Journal of Catalysis*, Vol. 141, pp. 9-20.

Sirijaruphan, A., J. G. Goodwin Jr. and R. W. Rice, 2004, "Effect of Temperature and Pressure on the Surface Kinetic Parameters of Pt/γ-Al_2O_3 during Selective CO Oxidation", *Journal of Catalysis*, Vol. 227, pp. 547-551.

Smith, J. M., 1981, *Chemical Engineering Kinetics*, McGraw-Hill, London.

Son, I. H., A. M. Lane and D. T. Johnson, 2003, "The Study of the Deactivation of Water-Pretreated Pt/γ-Al_2O_3 for Low-Temperature Selective CO Oxidation in Hydrogen", Short communication, *Journal of Power Sources,* Vol. 124, pp. 415–419.

Son, I. H., M. Shamsuzzoha and A. M. Lane, 2002, "Promotion of Pt/γ-Al_2O_3 by New Pretreatment for Low-Temperature Preferential Oxidation of CO in H_2 for PEM Fuel Cells", Research Note, *Journal of Catalysis*, Vol. 210, pp. 460-465.

Song, C., 2002, "Fuel Processing for Low-Temperature and High-Temperature Fuel Cells: Challenges and Opportunities for Sustainable Development in the 21st Century", *Catalysis Today*, Vol. 77, pp. 17-49.

Tanaka, H., S. Ito, S. Kameoka, K. Tomishige and K. Kunimori, 2003, "Catalytic Performance of K-promoted Rh/USY Catalysts in Preferential Oxidation of CO in Rich Hydrogen", *Applied Catalysis A: General*, Vol. 250, pp. 255-263.

Thormählen, P., M. Skoglundh, E. Fridell and B. Andersson, 1999, "Low-Temperature CO Oxidation over Platinum and Cobalt Oxide Catalysts", *Journal of Catalysis*, Vol. 188, pp.300-310.

Törncrona, A., M. Skoglundh, P. Thormählen, E. Fridell and E. Jobson, 1997, "Low Temperature Catalytic Activity of Cobalt Oxide and Ceria Promoted Pt and Pd: Influence of Pretreatment and Gas Composition", *Applied Catalysis B: Environmental*, Vol. 14, pp. 131-145.

Trimm, D. L. and Z. İ. Önsan, 2001, "Onboard Fuel Conversion for Hydrogen-Fuel-Cell-Driven Vehicles", *Catalysis Reviews-Science and Engineering*, Vol. 43 (1-2), pp. 31-84.

Uysal, G., 2005, *Effect of Carbon Dioxide and Water Vapor on Selective Carbon Monoxide Oxidation over Pt-Based Catalysts*, M. S. Thesis, Boğaziçi University.

Wang, D., Z. Hao, D. Cheng, X. Shi and C. Hu, 2003, "Influence of Pretreatment Conditions on Low-Temperature CO Oxidation over $Au/MO_x/Al_2O_3$ Catalysts", *Journal of Molecular Catalysis A: Chemical*, Vol. 200, pp. 229-238.

Wang, J. B., W. H. Shih and T. J. Huang, 2000, "Study of Sm_2O_3-Doped CeO_2/Al_2O_3-Supported Copper Catalyst for CO Oxidation", *Applied Catalysis A: General*, Vol. 203, pp. 191-199.

Wojciechowski, B. W. and N. M. Rice, 2003, *Experimental Methods in Kinetic Studies*, Elsevier, Boston.

Wootsch, A., C. Descorme and D. Duprez, 2004, "Preferential Oxidation of Carbon Monoxide in the Presence of Hydrogen (PROX) over Ceria–Zirconia and Alumina-Supported Pt Catalysts", *Journal of Catalysis,* Vol. 225, pp. 259-266.

Yan, J., J. Ma, P. Cao and P. Li, 2004, "Preferential Oxidation of CO in H_2-Rich Gases over Co-Promoted $Pt/\gamma\text{-}Al_2O_3$ Catalyst", *Catalysis Letters*, Vol. 93 (1/2), pp.55-60.

Zhdanov, V. P. and B. Kasemo, 2003, "The Effect of Oxide Formation on Bistability in CO Oxidation on Pt", *Journal of Catalysis*, Vol. 220, pp. 478-485.